NANYANG TECHNOLOGICAL UNIVERSITY

Applications of Convex Optimization in Plant-wide Control of a Solar Powered MDBR Water Recycling System

AVINASH VIJAY

SCHOOL OF ELECTRICAL AND ELECTRONIC ENGINEERING

2012

NANYANG TECHNOLOGICAL UNIVERSITY

Applications of Convex Optimization in Plant-wide Control of a Solar Powered MDBR Water Recycling System

AVINASH VIJAY

SCHOOL OF ELECTRICAL AND ELECTRONIC ENGINEERING

A THESIS SUBMITTED IN PARTIAL FULFILMENT OF
THE REQUIREMENTS FOR THE DEGREE OF
MASTER OF ENGINEERING

2012

Acknowledgments

I owe my deepest gratitude to my supervisor Assoc. Prof. Ling Keck Voon for his patience, support and encouragement. This thesis would not have been possible without his timely insights and suggestions. Regular inputs from members of The Institute of Environmental Science and Engineering (IESE), Li Jianfeng, Nyunt Wai and Prof. Tony Fane have also been very helpful during the course of my research. The staff at the Process Instrumentation Laboratory have to be acknowledged for their co-operation and technical expertise. I have been particularly fortunate during my graduate studies to have had the opportunity to communicate with a broad range of faculty, students, and visitors. I am also indebted to the National Research Foundation (NRF) for funding the grant that enabled the development of the water recycling plant under its Competitive Research Program (CRP).

Last, but by no means the least, I would like to thank my loved ones for their unyielding support and faith in my abilities. To them I dedicate this thesis.

Avinash Vijay

Table of Contents

List of Figures

List of Tables

Summary

The objective is to design a system which determines optimal operating points that will enable the solar powered Membrane Distillation Bio-Reactor (MDBR) water recycling plant to maximize the output produced while being self-sufficient. The system must optimize production rate during periods of adequate solar radiation and concentrate on survival of the essential micro-organisms in the MDBR during periods of inadequate solar radiation. Hence, uninterrupted plant operation during periods of unfavorable weather entails the management of a back up reserve. A balance has to be struck between minimization of power consumed and maximization of output produced to facilitate smooth operation. The challenge faced by this thesis is to translate these engineering objectives into convex optimization problems. This requires the modeling of plant dynamics to describe the relations between the variables of interest.

Control is implemented through a hierarchical framework consisting of the scheduling, supervisory and regulatory layers. The main focus of this thesis is on the scheduling and supervisory layers which require optimization. The scheduling layer decides how to cope with changes in weather conditions several days in advance. It manages system reserves based on

information available from the solar radiation prediction system to ensure continuous operation. The supervisory layer determines how the system will handle variation in solar radiation from dawn to dusk. Different control strategies and optimization problems required for this purpose have been considered. Since some relations in these problems are non-convex, the modifications required to solve them using convex optimization algorithms have also been discussed. Subsequently, simulations have been conducted to compare the performances of different strategies and to select the most desirable alternative. Illustrative examples have been provided for both layers to demonstrate the operation of the proposed system when subjected to different situations the plant is likely to encounter.

Chapter 1

Introduction

1.1 Motivation

Clean water is a scarce resource. This long squandered commodity will be in great demand in the future unless a cost effective means of producing clean water is established. Many advances have been made in the field of water reclamation in an effort to bridge the gap between supply and demand. Such advances have given rise to the creation of the Membrane Distillation Bio-Reactor (MDBR). Apart from 100% (theoretical) rejection of non-volatile organics, salts and biomass, MDBRs also offer lower carbon footprints and lower energy requirements in comparison to conventional distillation and pressure driven processes [1]. Further improvements can be brought about through optimization of the operating conditions. This thesis is dedicated to realizing the full potential of this possibility.

1.2 Static and dynamic approaches to MD/MBR process optimization

Optimization of Membrane Distillation (MD) and Membrane Bio-Reactor (MBR) processes in existing literature usually involves performing various experiments to analyze the effects of different parameters and determining the best combination from the collected data. They intend to determine a single stationary optimal operating point. These strategies will ensure that the water treatment system remains at that operating point irrespective of changes in any other external factors. Such operating points can be determined through experiments which vary different factors[2, 3, 4, 5] or through simulation [6]. Such methods are used also for design of MD and MBR units[7, 8, 9]. The basic difference between these publications and the current work is in the nature of the objective. The MDBR plant under consideration is solar powered. Hence, environmental conditions and available energy play an important role in its operation. Variation in external factors will have an effect in the performance of the MDBR plant and hence it has to manipulate control and management strategies to adapt to these changes. The publications mentioned above implicitly assume that supply or available energy will not be an issue and hence can afford to select a single operating point that is deemed optimal by their experiments.

One particular exception worth noting is the work of Chang et al. [10]. It is the closest in existing literature to the scope of the current work. They focus on optimizing the plant operating point with respect to the level of solar radiation. The Aspen custom modeler package is used to

describe the plant dynamics and optimize its operating conditions. The first major difference between [10] and the current work lies in the fact that they consider the operation of an MD unit which does not involve micro-organism activity. Secondly, it lays more emphasis on regulatory control and does not concern itself with the details of mathematical optimization. Finally, it does not consider the management of back up reserves required to ensure continuous operation. Analyzing the optimization solver being used to determine the operating points would provide interesting insights into how the system can be improved.

1.3 Main contributions

The main contributions of this thesis are:

- Design of the plant-wide optimization and control framework, demonstration its functional and dynamic performance
- Translation of semantic operational requirements into palpable control objectives that can be accurately and reliably solved using convex optimization algorithms
- Development of a supervisory optimizer to enable mode selection and real time optimization of operating conditions
- Development of a dynamic scheduler to determine optimal production strategies to maximize economic returns while minimizing the risk associated with changing environmental conditions

1.4 Outline

This thesis is composed of six chapters. Chapter 1 provides a general introduction, the specific contributions of this work and details regarding background information required to understand the contents presented in the chapters that follow. Broadly, Chapter 2 the background information on types of water reclamation, the MDBR concept and convex optimization. Chapter 3 describes the plant and the system under consideration. It presents the relations that govern different aspects of the plant and the hierarchical framework that will be used to control it. Chapters 4 and 5 explain how different layers of the control framework are designed and evaluated using simulations and real data. Preliminary results from these chapters were presented in the 11th International Conference on Control, Automation, Robotics and Vision, 2010 (ICARCV 2010)[11]. Two out of the three problem formulations elaborated in this thesis were presented at ICARCV. The third formulation presented in this thesis has been shown to be more effective than the others presented at ICARCV. Details of the modifications required to make use of convex optimization have also been discussed in this thesis in addition to the content in [11]. Chapter 6 presents a summary of the conclusions arrived from the work done and recommends directions for further research.

Chapter 2

Background

Introductions to the main aspects of this work have to be presented before proceeding to the design and evaluation segments. This section serves as an prelude to familiarize the uninitiated reader to the tools and technologies associated with this work. It begins by providing a general discussion of various types of water reclamation systems and a detailed discussion of the specific technology under consideration: Membrane Distillation Bio-Reactor (MDBR). The MDBR process integrates membrane distillation into a submerged membrane bio-reactor. Hence, to enhance comprehension, reviews of the Membrane Distillation and Membrane Bio-Reactor processes are presented before the discussion of the MDBR. This is followed by brief explanations of solar photovoltaics, the elements of convex optimization and plant-wide control.

2.1 Different types of water reclamation systems

Recognition of wastewater as a potential resource has inspired the development of a plethora of technologies to recycle wastewater. Techniques developed range from simple systems for residential use to advanced variants for large-scale water treatment.

2.1.1 Simple treatment systems

Elementary systems consist of a two stage process involving coarse filtration and disinfection. Coarse filtration usually uses a screen which is a device with openings, generally of uniform size, to retain solids found in the influent wastewater. Disinfection is done through the usage of either chlorine or bromine. Such systems are designed to meet standards that are not severe. They are suitable for non-potable reuse of water from showers, hand basins and laundry troughs as discussed in[12, 13].

2.1.2 Physico-chemical systems

The quality obtained from physico-chemical systems is observed to be better than that produced by the simple systems described in the previous section[14]. Such systems are usually based on depth filtration where the liquid is passed through a filter bed consisting of a granular or compressible filter medium. Complex variants involve coagulation or advanced oxidation processes which are discussed in the following sections.

2.1.2.1 Coagulation–flocculation

This two stage process is used when the nature of the colloidal suspension does not permit them to be separated via conventional physical methods such as sedimentation or settling. Coagulation is usually achieved through addition of chemical coagulants. These coagulants(aluminum or ferric salts) promote destabilization of the colloid dispersion. Subsequent agglomeration of the resulting particles into larger aggregates is realized through flocculation as discussed in[15, 16, 17].

2.1.2.2 Advanced oxidation processes

Advanced oxidation processes make use of the hydroxyl free radical as a strong oxidizing agent. These processes can handle compounds that cannot be oxidized by traditional oxidizing agents such as oxygen, ozone and chlorine. The required hydroxyl free radical could be produced through the usage of ozone along with ultraviolet radiation[18, 19] or hydrogen peroxide[20].

2.1.3 Pressure driven membrane processes

Conventional treatment systems do not make use of a single process separation for all the dissolved constituents at a molecular or ionic level. Pressure driven membrane processes offer such a solution while operating at ambient temperature and without any chemical addition. Such processes have some associated drawbacks such as membrane fouling and membrane surface degradation. Nevertheless, these issues can be tackled through proper

pretreatment of effluents, selection of appropriate membrane materials and optimization of operating conditions such as temperature, flow rate etc. Table 2.1 gives the application of various membrane processes for the separation of different types of contaminants.

Table 2.1: Membrane applications for different contaminants[21]

Contaminant species	Membrane process
Particulate matter and suspensions	Microfiltration (MF)
Colloidal impurities	Microfiltration (MF)
High molecular weight organics	Ultrafiltration (UF)
Middle molecular weight organics	Ultrafiltration (UF)
Low molecular weight organics	Nanofiltration (NF), Reverse Osmosis
Multivalent ionic solutes	Nanofiltration (NF), Reverse Osmosis

All of the membrane processes in Table 2.1 make use of selectively permeable synthetic barriers. The desired components are allowed to pass through the barrier to be collected as the permeate. The transport of these components is effected through the application of a suitable driving force : hydrostatic pressure.

All membrane separation processes are based on the separation of a mixture of substances through the usage of a selective thin film. The presence of a transmembrane force gives rise to preferential transfer of one or more constituents of the feed. Membrane pore size decides the degree of selectivity. An overview of the main pressure driven membrane separation processes for which water is the permeate product is presented in Figure 2.1.

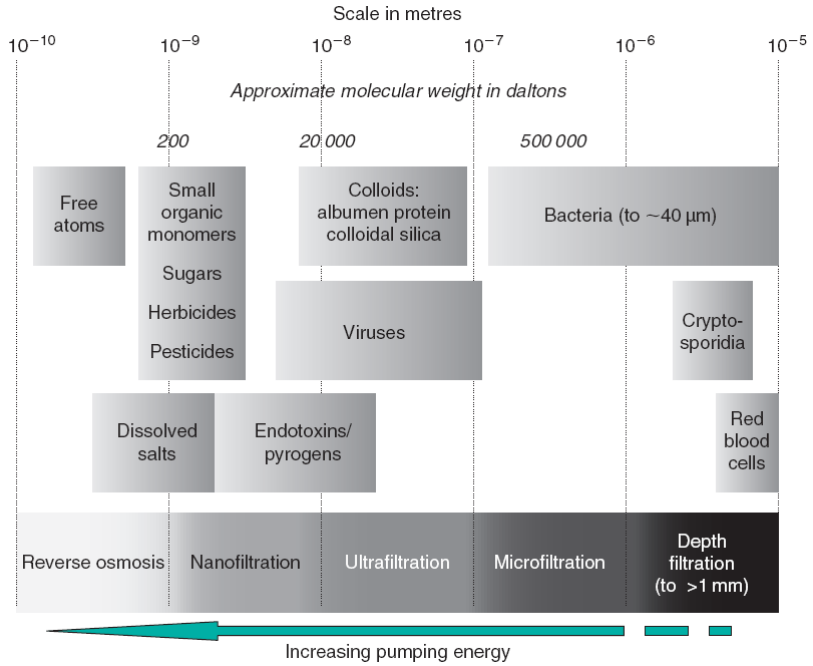

Figure 2.1: Overview of pressure driven membrane separation processes[22]

2.1.4 Membrane Distillation

Membrane Distillation (MD) was first patented and introduced almost half a century back[23, 24]. But enthusiasm towards this technology waned since its production levels were not able to match up to that of its counterparts based on reverse osmosis. Later, the advent of improved membranes and modules contributed towards a renewed interest in MD in the 1980s[25]. Extensive research has been done on this subject since its introduction in 1963. MD has now been developed into a cost effective separation process that can operate with low grade waste heat.

The Membrane Distillation process involves the usage of membranes which are microporous and hydrophobic. These membranes are brought in contact with a heated aqueous solution (feed solution) on one side. A

vapor-liquid interface is created at each pore entrance since the hydrophobic nature of these membranes prohibits any mass transfer in the liquid phase. Figure 2.2[26]shows how these vapor-liquid interfaces are supported at the pore openings.

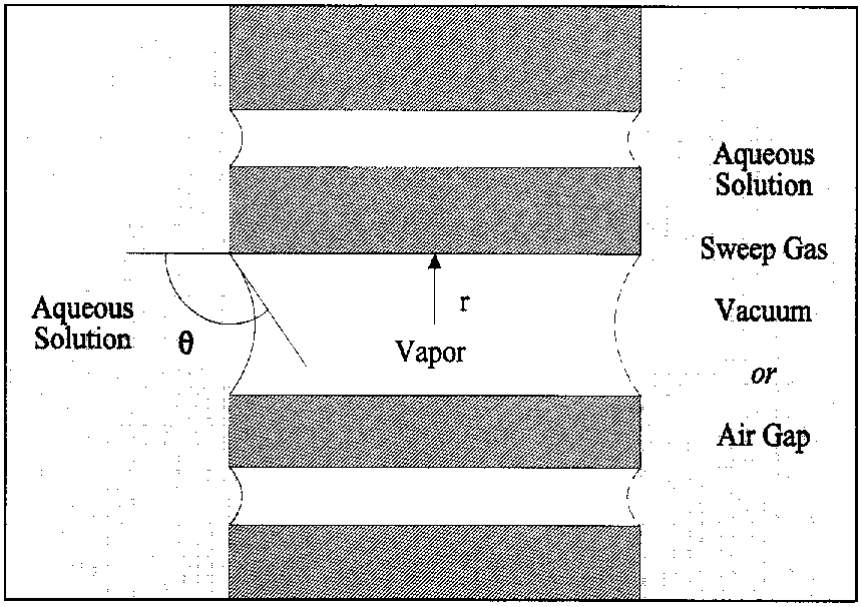

Figure 2.2: Vapor-Liquid interface in MD[26]

MD configurations usually differ in the ways in which a vapor pressure gradient is imposed across the membrane. In the most commonly used configuration, Direct Contact Membrane Distillation (DCMD), the permeate side of the membrane is allowed to be in direct contact with a condensing fluid. A condensing surface can also be used instead of the condensing fluid. This surface could be separated from the membrane by means of an air gap (AGMD), vacuum (VMD) or a sweep gas (SGMD). All of these configurations have been illustrated in Figure 2.3.

Irrespective of the configuration used, a mixture of water and volatile

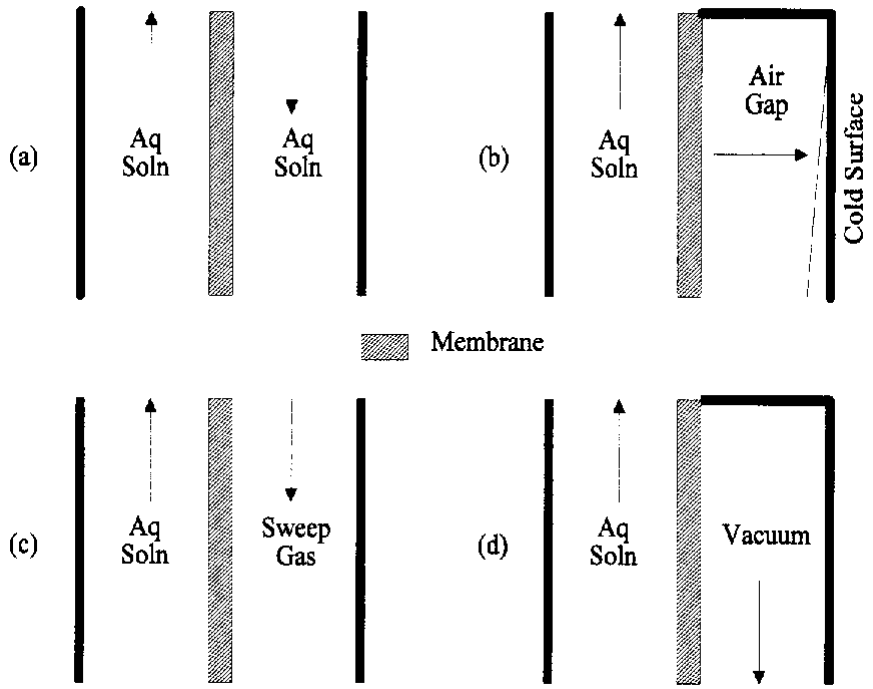

Figure 2.3: MD Configurations:(a)DCMD (b) AGMD (c) SGMD (d) VMD[26]

solutes (if present) evaporates from the liquid—vapor interface on the feed side. This mixture then diffuses across the membrane to be condensed and/or removed from the module on the permeate side.

The membrane distillation process offers many advantages over other separation techniques. Since it is based on volatility and not pore size (like reverse osmosis and ultrafiltration), 100%(theoretical) rejection of ions, macromolecules, colloids, cells and other non-volatiles is possible. MD supports lower operating temperatures in comparison to the distillation process. Hence lesser heat is required. This factor allows the MD process to be coupled with alternative sources of energy from solar or geothermal plants.

Operating pressure is also found to be relatively lower when compared to pressure driven techniques like reverse osmosis. This results in a decrease in equipment cost and an increase in process safety. Pore sizes encountered in MD processes are relatively larger than those encountered in reverse osmosis. Thus they are less likely to get clogged. Membranes in the MD process do not have to be selective like the membranes used in processes like pervaporation. They only have to serve as a barrier at the liquid-vapor interface.

2.1.5 Membrane Bio-Reactor

First commercial Membrane Bio-Reactors (MBRs) surfaced in the early 1970's and were used mainly for ship-board sewage treatment[27]. These systems were able to couple an activated sludge process with a membrane separation system to produce disinfected water of high quality. They were prevalently used in japan for domestic waste water treatment during the 1980s. In recent times, membrane bio-reactors have gained importance in the water treatment industry due to significant reductions in cost and introduction of more stringent effluent standards. The main features to be considered during the use of membrane bio-reactors are:

- Membranes and the membrane process
- MBR configurations
- Membrane fouling

The significance of the different types of membranes used has been highlighted in Section 2.1.3. Apart from the nature of the membranes themselves, the configuration in which they are used also plays a vital role in the separation process. Membrane Bio-Reactors can be broadly classified into two categories according to their configurations as shown in Figure 2.4[22]. The classifications are based on the location of its functional units: the biological unit and the membrane unit. In the side stream configuration, the membrane unit is separated from the biological unit or the bio-reactor. The sludge from the bio-reactor is transferred to the membrane unit. After the permeate passes through the membrane, the concentrated sludge is returned to the bio-reactor. The re-circulation pump has to generate both the cross flow velocity and the trans membrane pressure required for the process. This results in higher energy consumption. Hence in an effort to reduce the amount of energy consumed, the immersed configuration was introduced in 1989[28]. Here, the membrane unit is submerged inside the bio-reactor. The need for a re-circulation pump had thus been eliminated. Only a suction pump was required to create the transmembrane pressure. In some cases associated with low filtration fluxes, gravity itself can be utilized to provide this driving force.

One of the main factors which hinder the practical application of MBRs is fouling. Membrane fouling is a process which involves particle deposition upon the membrane surface or inside the membrane pores[29]. Fouling results in decrease in membrane performance and can cause severe flux decline. Severe membrane fouling may require intense chemical cleaning and in some cases replacement of the entire membrane. The three-stage process,

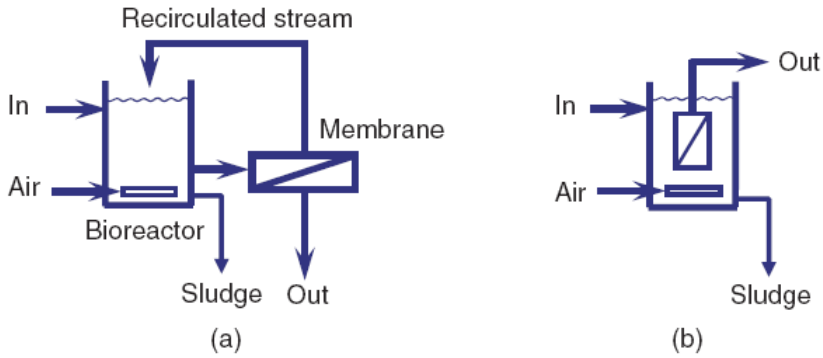

Figure 2.4: MBR configurations: (a) Side stream configuration (b) Immersed configuration[22]

wherein various mechanisms prevail, is summarized in Figure 2.5[30]. The mechanisms involved in this process are beyond the scope of this Thesis and hence will not be discussed.

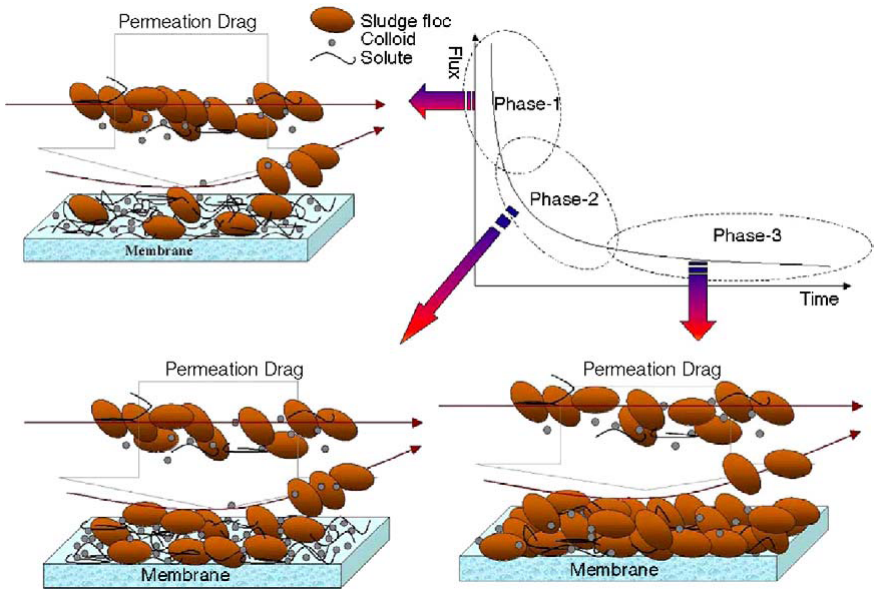

Figure 2.5: Illustration of initial cake layer formation[30]

The effects of fouling can be removed through application of physical and chemical methods. Relaxation and back washing are the most common physical methods in use. Relaxation involves breaks or pauses in filtration. Back washing involves the reversal of permeate flow direction. With the passage of time, the effectiveness of physical cleaning methods decreases. This leads to the accumulation of solute particles. Eventually these particles form a matrix that binds them together resulting the formation of an irreversible fouling layer. Chemical cleaning agents like sodium hypochlorite, citric acid and oxalic acid are required in such situations[29].

Despite membrane fouling MBRs have become attractive alternatives to conventional waste water treatment processes by virtue of their associated benefits: small footprint, excellent effluent quality and high disinfection capacity[22]. MBRs also have shorter start up times and produce lesser sludge than conventional techniques and can be easily incorporated into existing water treatment plants. Thus they have immense potential to become the technology of choice in the years to come.

2.1.6 Membrane Distillation Bio-Reactor

The Membrane Distillation Bio-Reactor is a nascent technology that has the potential to be widely adopted as an efficient means of water reclamation. Only three papers have been published on this subject and none of them deal with issues related to the design and analysis of plant-wide control systems for MDBR water recycling plants. Broadly, they cover the introduction of the novel concept and experimental studies related to its performance.

The first paper on this subject by Phattaranawik et al. [1] describes the idea behind the water treatment process involving the MDBR. They propose that the conventional pressure driven membranes in MBRs can be replaced by membrane distillation. This paper explains the problems associated with conventional Microfiltration(MF)/Ultrafiltration(UF)-MBR systems and how the usage of the MDBR can help avoid them.

In the second paper[31], Phattaranawik et al. proceed to demonstrate how the MDBR concept can be implemented as a lab-scale prototype. Experimental studies of both tubular and flat sheet membranes have been presented. Their paper will serve as a useful reference for the design of MDBR modules. They highlight issues such as the importance of the hydrodynamics of the permeate stream and the need to optimize energy recovery to improve thermal efficiency.

The third paper by Khaing et al.[32] evaluates the feasibility of the use MDBRs in the petrochemical industry. Tests conducted indicated that the permeate quality met the standards set by NEWater of Singapore. The results show that the hydrophobic membranes displayed good separation characteristics during the entire course of the study. They were also able to show that decline in membrane permeability due to inorganic fouling can be recovered by cleaning.

The Membrane Distillation Bio-Reactor (MDBR) was introduced in an attempt to mitigate two distinct disadvantages faced by UF/MF-MBR systems which have been used extensively in the water treatment industry[31]. As the membrane only retains large colloids, biomass and some macrosolutes , the product contains low molecular weight solutes . Such solutes can

affect downstream processes like disinfection and purification by reverse osmosis. Another problem stems from the equality of the hydraulic retention time and the retention time of the organic substrate. Hence, slowly degraded waste products can pass out of the MF/UF-MBR before they can be degraded. Further, the incidence of viable-but-not-culturable (VBNC) bacteria could compromise the performance of UF/MF-MBR systems since they can be smaller than the pore sizes usually encountered.

Attempts to alleviate these issues through the usage of Nanofiltration (NF) along with submerged MBRs[33] resulted in very low fluxes due to the low transmembrane pressures (TMP) available for NF. The MDBR makes use of a different particle rejection mechanism to resolve these issues. It integrates a membrane distillation module into a submerged membrane bio-reactor as shown in Figure 2.6 [1]. The thermally driven membrane distillation process allows only volatile solutes to pass thorough. As long as the pores of the hydrophobic membrane are not wetted internally, MD is an efficient and effective process. It offers 100% theoretical rejection of non-volatile organics, salts and biomass[1]. Since MD requires slightly elevated operating temperatures, thermophilic bacteria are preferred over mesophilic bacteria in MDBRs.

In summary, the MDBR combines the potential benefits of both MD and MBR with some added advantages such as shorter start up times and easier online conductivity analysis.

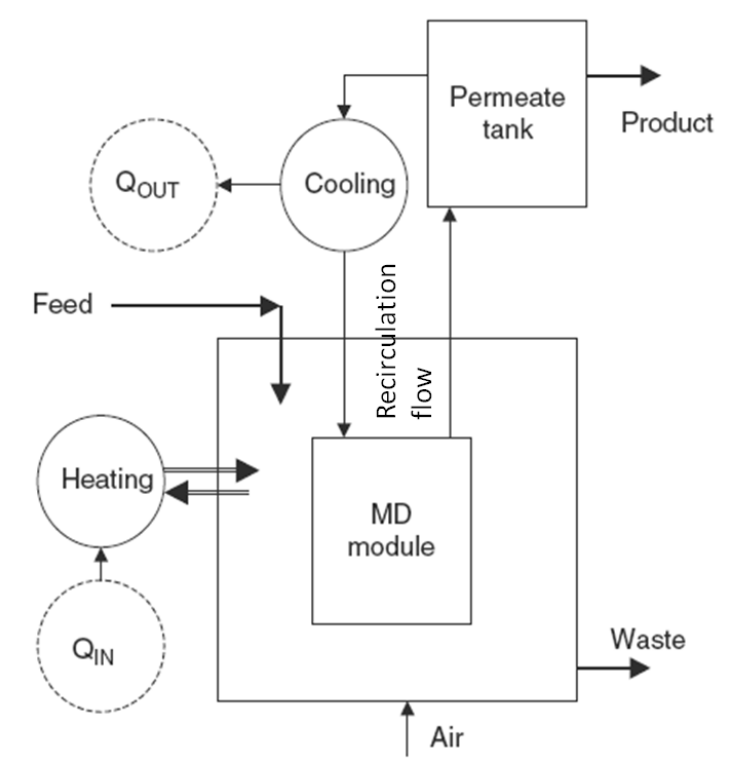

Figure 2.6: Schematic arrangement of MDBR(modified from [1])

2.2 Solar Photovoltaics

Photovoltaics (PV) is generally based on the development of an electric voltage, between two electrodes attached to a solid or liquid object, upon the introduction of light into this system. These devices are also known as solar cells. A solar cell uses the photovoltaic effect, in order to produce electricity. Practically all photovoltaic devices incorporate a semiconductor p-n junction between the base and emitter across which the voltage is developed. Figure 2.7 shows a schematic of a typical photovoltaic solar cell.

In most cases either boron or phosphorous impurities are used to dope the junction to result in an electric field. Energy from the photons in light,

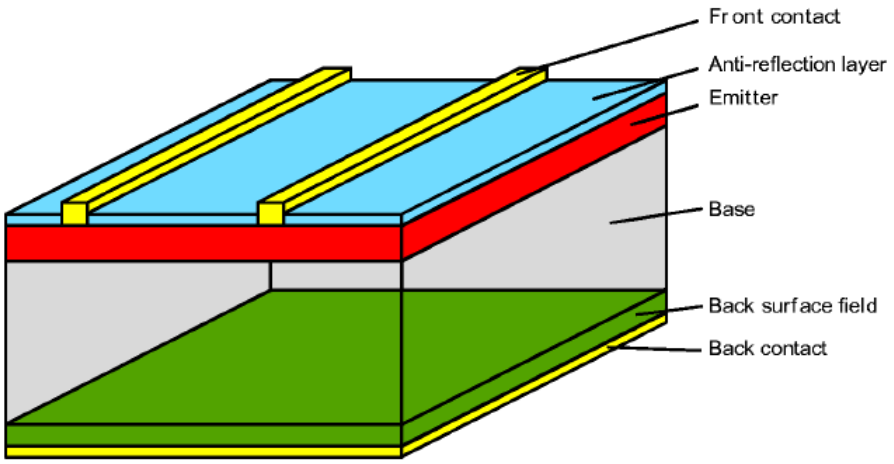

Figure 2.7: Schematic of typical solar cell[34]

upon entering the solar cell, lead to the creation of charge carriers which are separated by the electrical field. A voltage thus generated at the external contacts, can cause a current to flow when a load is connected to them. The photocurrent, i.e. the current generated in the solar cell, is proportional to the radiation intensity as shown in Figure 2.8.

Many semiconductor materials are suitable for creating solar cells. The most commonly used material is silicon. This kind of silicon is known as solar grade silicon. Bulk silicon is separated into different categories according to crystal type and size in the resulting ingot, ribbon or wafer. The types of silicon solar cells can be divided into three categories: monocrystalline, polycrystalline and amorphous silicon cells. Other materials, such as cadmium telluride, copper-indium selenide, gallium arsenide multi-junction, organics or polymers, are also used to produce solar PV cells. But they are less common.

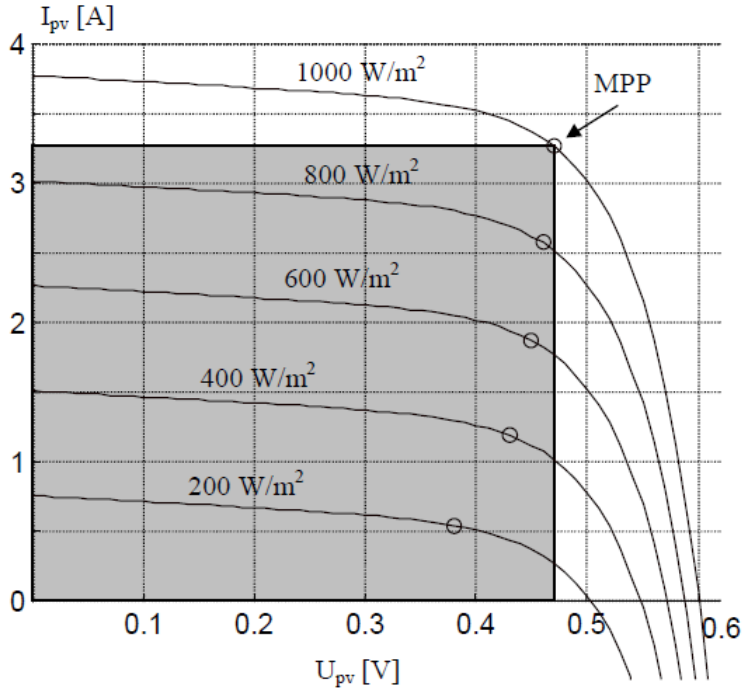

Figure 2.8: IV-curves for a PV-cell at different insolations [35]

2.3 Convex optimization

Convex optimization is being used in a multitude of engineering applications due to its capacity to efficiently solve practical engineering problems. Although the mathematics involved in convex optimization has been studied for nearly a century, its use in engineering applications was fuelled mainly by the development of interior point methods[36, 37]. Towards the 1980s it was recognized that these methods[38, 39] could be used to solve non-linear convex optimization problems almost as easily as linear programs. Most of the content present in this section is based on the book, Convex Optimization by Boyd and Vandenberghe[40].

2.3.1 Mathematical optimization

Convex optimization is a subfield of mathematical optimization. Hence it is important to understand the structure of a mathematical optimization problem:

$$\begin{aligned} \underset{x}{\text{minimize}} \quad & f_0(x) \\ \text{subject to} \quad & f_i(x) \leq b_i \quad i = 1, \ldots, m \\ & h_j(x) = c_j \quad j = 1, \ldots, p \end{aligned} \tag{2.1}$$

It consists of three factors: an optimization variable, an objective function and a set of constraints. Here the vector $x = (x_1, \ . \ . \ . \ , x_n)$ is the optimization variable of the problem, the solution of the optimization problem results in values for each one of its components. The function $f_0 : R^n \rightarrow R$ is the objective function, this represents the quantity or the function that has to be minimized. The functions $f_i : R^n \rightarrow R \forall i = 1, \ldots, m$ and $h_j : R^n \rightarrow R \forall j = 1, \ldots, p$ are the inequality and equality constraint functions respectively. The constants $b_1, \ldots, b_m$, and $c_1, \ldots, c_p$are the limits, or bounds, for the constraints. A vector x^* is called optimal, or a solution of the problem, if it has the smallest objective value among all vectors that satisfy the constraints: for any z with $f_1(z) \leq b_1, \ . \ . \ . \ , f_m(z) \leq b_m$, we have $f_0(z) \geq f_0(x^*)$.

A convex optimization problem is one where the functions $f_0, ..., f_m$ are convex and the functions $h_1, ..., h_p$ are affine. These restrictions on the objective function and constraints are the factors which differentiate convex optimization problems form those described in Section 2.3.1. The feasible

region of a convex optimization problem is always a convex set. Hence, in simple terms, convex optimization can be viewed as a process which minimizes a convex function over a convex set. A discussion of convex sets, affine sets and convex functions has been provided below to help understand the elements of convex optimization.

2.3.2 Convex analysis

2.3.2.1 Convex sets

A set is said to be convex when the line segment joining any two distinct points inside the set is also within the set. Mathematically the line segment between any two points $x_1$and x_2 can be represented as:

$$\theta x_1 + (1-\theta)x_2 \forall \theta \in [0,1]$$

Hence, a set C is said to be convex, if for any $x_1, x_2 \in C$ and $x_1 \neq x_2$, we have $\theta x_1 + (1-\theta)x_2 \in C$. The difference between a convex and non-convex set has been illustrated in Figure 2.9.

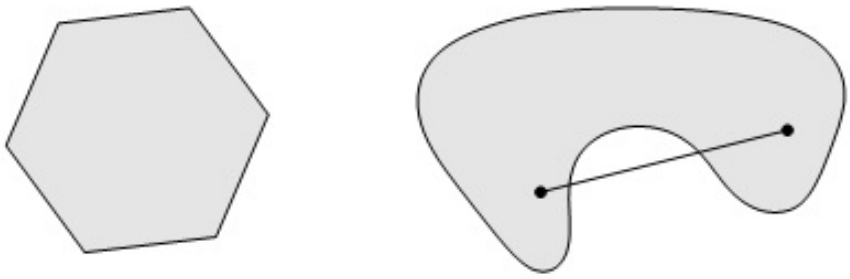

Figure 2.9: Difference between a convex set (left hand side) and a non-convex set (right hand side)[40]

2.3.2.2 Affine sets

A set is said to be affine when the line between passing through any two distinct points inside the lies within the same set. The main difference between convex sets and affine sets is the facts that convex sets have to contain only the portion of the line in between the two points in consideration, where as affine sets have to contain the entire line itself. Hence, all affine sets are convex.

2.3.2.3 Convex functions

For any real valued function to be convex, it has to satisfy two conditions. Firstly, its domain has to be a convex set. Secondly, its epigraph should also be a convex set. This concept can also be understood graphically. The line joining any two points on the curve representing a convex function is always above the curve itself as shown in Figure 2.10.

Figure 2.10: Graph of a convex function[40]

Another way of representing the above mentioned condition is:

$$f(\theta x + (1-\theta)y) \leq \theta f(x) + (1-\theta)f(y)$$

A function is said to be concave if $(-f)$ is convex.

2.3.3 Algorithms

2.3.3.1 Unconstrained minimization

The "simplest" form of a convex optimization problem is the unconstrained minimization problem. Its consists only of an objective function:

$$\underset{x}{\text{minimize}} f(x)$$

where f is convex and twice continuously differentiable. A finite optimal value $p^* = inf_x f(x)$ has to be attained at the end. Hence unconstrained minimization methods can be viewed upon as methods which produce a sequence of points $x^{(k)}$, $k = 0, 1, ...$ belonging to the domain of f such that $f(x^{(k)}) \rightarrow p^*$. This sequence of points will be referred to as the minimization sequence.

2.3.3.2 Descent methods

Descent methods produce the minimization sequence by using the following relation:

$$x^{(k+1)} = x^{(k)} + t^{(k)} \Delta x^{(k)}$$

where $t^{(k)} > 0$ (except when $x^{(k)}$ is optimal) is the step size or scale factor, $\Delta x^{(k)}$ is a vector in R^n called the step or search direction (even though it need not have unit norm), and k = 0, 1, . . . denotes the iteration number.

Since these algorithms are descent methods, they are designed such that the next sequence in the algorithm has to satisfy,

$$f(x^{(k+1)}) < f(x^{(k)})$$

except when $x^{(k)}$ is optimal. This implies that for all k we have $x^{(k)} \in S$, the initial sublevel set, and in particular we have $x^{(k)} \in \text{dom } f$, or domain of f. From convexity we know that $\nabla f(x^{(k)})^T(y{-}x^{(k)}) \geq 0$ implies $f(y) \geq f(x^{(k)})$, so the search direction in a descent method must satisfy $\nabla f(x^{(k)})^T x^{(k)} < 0$, i.e., it must make an acute angle with the negative gradient. We call such a direction a descent direction (for f, at $x^{(k)}$). Having explained these, we can move to the general descent method. In this method we assume that, given a starting point $x^{(k)} \in \text{dom } f$, the following steps are repeated until the stopping criterion is satisfied.

1. Determine a descent direction $\Delta x^{(k)}$.
2. *Line search.* Choose a step size $t^{(k)} > 0$.
3. Update. $x^{(k+1)} = x^{(k)} + t^{(k)}\Delta x^{(k)}$.

where *Line search* is the process of determining a suitable value for the scale factor $t^{(k)}$. This can be done through either an exact line search which solves a minimization problem,

$$t^{(k)} = argmin_{s \geq 0} f(x^{(k)} + s\Delta x^{(k)})$$

or through an inexact approximation to minimize f along the ray $\{x^{(k)} + t^{(k)}\Delta x^{(k)} | t^{(k)} \geq 0\}$, or even to just reduce f "enough". More details can be found in [40]. For notational simplicity, the superscript (k) will be

dropped from this point onwards in this section. The more interesting part of the algorithm is the determination of the descent direction. This is what differentiates the types of descent methods used. In the gradient descent method, the negative gradient is used:

$$\Delta x = -\nabla f(x)$$

In the steepest descent method, the unit-norm step with most negative directional derivative is used:

$$\Delta x_{sd} = argmin\{\nabla f(x)^T v |\, \|v\| = 1\}$$

In the newton method, a quadratic approximation is used to calculate the newton step as:

$$\Delta x_{nt} = -\nabla^2 f(x)^{-1} \nabla f(x)$$

and the stopping criterion is defined as $\lambda^2/2 \leq \epsilon$, where λ or the newton decrement is,

$$\lambda(x) = \left(\nabla f(x)^T \nabla^2 f(x)^{-1} \nabla f(x)\right)$$

2.3.3.3 Equality constrained minimization

Equality constraints in convex optimization are of the form $\{x|Ax = b\}$. These are represented as,

$$\{x|Ax = b\} = \{Fz + \hat{x}|z \in R^{n-p}\}$$

where $\hat{x}$ is (any) particular solution and the range of $F \in R^{n\times(n-p)}$ is the null space of A (rank $F = n - p$ and $AF = 0$). Hence the reduced problem becomes,

$$\underset{z}{\text{minimize}} f(Fz + \hat{x})$$

which is an unconstrained minimization problem with variable $z \in R^{n-p}$.

2.3.3.4 Newton method with equality constraints

The newton step Δx_{nt} of f at feasible x is given by the solution v of

$$\begin{bmatrix} \nabla^2 f(x) & A^T \\ A & 0 \end{bmatrix} \begin{bmatrix} v \\ w \end{bmatrix} = \begin{bmatrix} -\nabla f(x) \\ 0 \end{bmatrix}$$

The newton decrement for an equality constrained problem is,

$$\lambda(x) = (\Delta x_{nt}^T \nabla^2 f(x) \Delta x_{nt})^{1/2} = (-\nabla f(x)^T \Delta x_{nt})^{1/2}$$

2.3.3.5 Inequality constrained minimization and Interior point method

Such problems are of the form:

$$\begin{aligned} \underset{x}{\text{minimize}} \quad & f_0(x) \\ \text{subject to} \quad & f_i(x) \leq 0, \quad i = 1, ..., m \quad (A1) \\ & Ax = b \end{aligned}$$

where f_i are convex and twice continuously differentiable, $A \in R^{p \times n}$ with rank $A = p$. We assume that the optimal solution p^* is finite and that the problem is strictly feasible. In other words, there exists $\tilde{x}$ with

$$\tilde{x} \in \text{ dom } f$$
$$f_i(\tilde{x}) \leq 0, i = 1, ..., m$$
$$A\tilde{x} = b$$

The problem described above can be reformulated as,

$$\begin{aligned} \underset{x}{\text{minimize}} \quad & f_0(x) + \Sigma_{i=1}^{m} I_-(f_i(x)) \\ \text{subject to} \quad & Ax = b \end{aligned}$$

where $I_-(u) = 0$ if $u \leq 0, I_-(u) = \infty$ otherwise; is the indicator function of R_-. The indicator function can be approximated through the use of the logarithmic barrier function. The problem then takes the form,

$$\begin{aligned} \underset{x}{\text{minimize}} \quad & f_0(x) + \Sigma_{i=1}^{m} - (1/t) log(-f_i(x)) \\ \text{subject to} \quad & Ax = b \end{aligned}$$

The objective here is convex, since $-(1/t)log(-u)$ is convex and increasing in u, and differentiable. Newton's method can be used to solve it. Since the problem presented above is still only an approximation of the original problem , so one needs to consider how it approximates a solution of the original problem (A1) from the beginning of Section 2.3.3.5. It has been observed that the quality of the approximation improves as the parameter t increases. On the other hand, when the value of t is large, the function $f_0(x) + \Sigma_{i=1}^{m} - (1/t) log(-f_i(x))$ is difficult to minimize by Newton's method.

Its Hessian varies rapidly near the boundary of the feasible set. This problem can be handled by solving a sequence of problems while increasing the value of t at each step. The solution of the problem for the previous value of t is used as the starting point for each Newton minimization. This process is known as the interior point method.

2.3.4 Handling and approximating non convex problems

Convex optimization methods have the advantage of always being close to the global optimal and always being fast to compute. But, this advantage ceases to exist when the optimization problem is not convex. For non convex problems, we can use either local optimization methods which are fast, but don't necessarily have to find the global solution or, global optimization methods which can find the global solution but are not usually fast (rather slow in a lot of cases). In general such problems are handled either through the use of sequential convex programming or through the use of convex relaxations.

Sequential Convex Programs (SCP) use a local optimization method for non convex problems that leverages convex optimization. In this method, convex portions of the non convex problems are used. In other words, the original problem is substituted by a convex approximation over a specific trust region. These trust regions are usually bounding boxes in the solution space. Once an "optimal" (optimal for the approximation) solution for the current trust region is obtained, the next trust region is formed around

the "optimal" solution determined and the process is repeated. SCP is a heuristic. It has a set of drawbacks: it can fail to find an optimal or even a feasible point and the results usually depend heavily on the starting point used. But, it is often found to work well to find a good objective value even though it may not be optimal.

Convex relaxations involve the usage of approximate convex functions over the entire solution space. As long as the approximation sufficiently resembles the original non convex problem, the solutions obtained provide practical value even if they are not globally optimal. An important factor to be kept in mind while obtaining these approximations is that, all the conditions that satisfy the approximations must satisfy the original non-convex constraints, otherwise the optimization results will violate the actual constraints. Hence, analysis of the constraints and the "closeness" of the approximation is required while using this method.

2.3.5 Benefits of using convex optimization

The main advantage of identifying and framing a problem as a convex optimization problem lies in the fact that all local optima are global. Hence, exhaustive searches are not necessary. Since convex analysis is a well developed branch of mathematics, convex optimization has the luxury of having tight lower bounds on the optimal value of a problem. Convex analysis also offers reliable indicators of infeasibility and unboundedness. In some special cases, the structure of the problem can be exploited to drastically decrease computation time.

2.4 Plant-wide control framework

Plant-wide control essentially refers to the control of the whole plant in its entirety. Hence synthesis of plant-wide control is the design of a control system that can enforce all the required control objectives in an optimal fashion. The design of such systems involves more effort than that required for control of individual units because of the magnitude of the problem. The presence of interactions between different components only complicates issues further. Local control actions can also have adverse long term effects throughout the plant. The concept of plant-wide control and the design of controllers for this purpose has attracted a lot of attention over the years. As a result, many efforts to offer a formal framework have been made[41, 42, 43, 44].

In general, the design of plant-wide control systems can be summarized as follows[42]: Given a process flowsheet, a vector of process disturbances, that are expected to impact the operation of the plant, a vector of possible measurements, and a vector of available manipulated inputs,

- Identify the control objectives
- Select the necessary measured variables
- Select the requisite manipulated variables
- Select controller configuration and controller type

so that the resulting control system can meet the operating objectives of the plant in an optimal manner. The control objectives are usually a direct consequence of the plant and the process under consideration.

2.4.1 Hierarchical framework

Design of a centralized monolithic unit to handle all of the control objectives is usually plausible only when the plant model, dynamics and control objectives are reasonably simple and well defined. Most practical situations involve complex non-linear multivariable processes which do not come under this category. Hence, the main control problem is usually divided into a set of simpler, hierarchically formulated sub-problems. Each sub-problem is assigned a separate layer of control to enhance performance and reliability. These layers or sub problems can be characterized by different time scales. The differences in granulation of time are handled well without increasing the computational load on control in the hierarchical structure. This scheme also allows the system to combine the use different tools and methods that can be tailored to the needs of each specific sub-problem. Figure 2.11 presents the generic functional constituents of a hierarchical plant-wide control structure. The three layers of a typical hierarchical control structure differ from from each other in terms of the function they perform and in terms of the time scales in which they operate in. They are presented in increasing order of their timescales:

- Regulatory layer (Minutes)
- Supervisory layer (Hours)
- Scheduling layer (Days)

The top layer or the scheduling layer governs the economic criteria set by the plant management and operates in a time scale in the order of

days. The supervisory layer takes care of optimizing control conditions. It determines the optimal operating conditions depending upon the plant dynamics. The supervisory layer usually operates in a shorter time scale in the order of hours. Finally, the regulatory layer minimizes any deviations from the operating conditions specified by the supervisory layer. This layer operates in the shortest time scale of the three in the order of minutes or seconds.

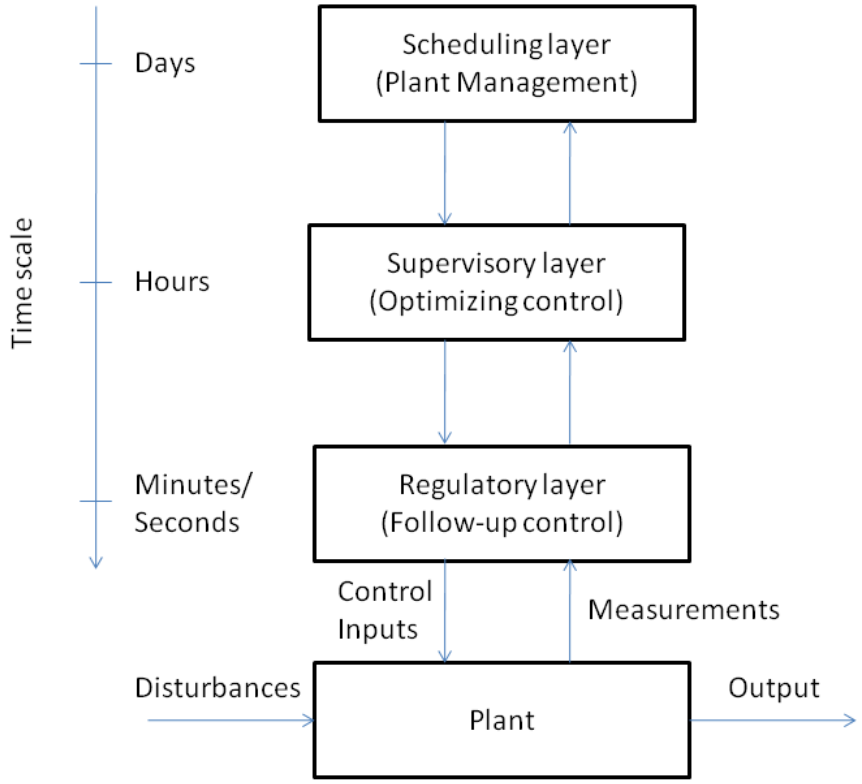

Figure 2.11: Hierarchical plant-wide control structure

2.4.2 Issues in plant-wide control

Traditionally, processing units in a plant are connected in either series or parallel configuration only. In this situation, the units behave essentially as if they were isolated and each unit simply sees upstream units as sources of disturbances. With passage of time, plants have become more integrated, i.e. raw materials and energy are recycled to upstream units for economic and environmental reasons. The units have stronger interactions due to the presence of such recycling. In particular, disturbances no longer simply propagate downstream, but are fed back from downstream units to upstream units. Hence, the behavior of each unit within the overall system may be highly different from the behavior of the same unit when operated in isolation.

The operating conditions of the process do not remain the same when recycling is introduced. The open-loop characteristics of the process will change. But, the effects of these changes are usually highly process specific, and it is difficult to draw any general conclusions. Morud and Skogestad [45] explain that, small changes, or disturbances, will be fed back by the recycle flow, thereby introducing a feedback effect. Gilliland et al.[46] discuss that recycling may give rise to two different types of instability, and termed these 'snowball' instability and 'oscillatory' instability, respectively. From a dynamic systems perspective, the snowball and oscillatory instabilities correspond to real and complex poles in the complex RHP, respectively.

It is therefore a challenging task to design of effective plant-wide control systems with increase in complexity and interactions between units. This

section is based on the content in [47], where more details on this topic can be found.

2.5 Chapter summary

This chapter provides an overview of the background information required for the different aspects of this thesis. Different types of water reclamation systems are discussed, ranging from simple two stage flitration systems to the more complex MDBR under consideration. This is followed by a discussion of solar photovoltaics to provide information on solar power generation and how irradiation affects current and voltage. The next two sections concerning convex optimization and plant wide control are related to computation, algorithms and decision making in control strategies. These aspects are not related to hardware but rather control and optimization. A brief explanation of convex optimization, algorithms and methods to handle non convex terms have been presented. The final section of the chapter moves on to plant-wide control, the significance of the framework used and the issues associated with plant-wide control. Thus the reader can move on to the specific requirements of the MDBR plant under consideration.

Chapter 3

The Solar Powered MDBR Plant

The water recycling system considered in this work is based on the plant being developed by Nanyang Technological University, Singapore. It sets itself apart by being one of the first plants to make use of solar energy to operate an MDBR system. This chapter first divides the plant into functional subsystems in Section 3.1. It then proceeds to explain how these subsystems work together to facilitate plant operation. Section 3.3 presents the mathematical relations used to model the dynamics of the plant and the basis upon which they are validated. The final sections deal with the actual operational needs and the control framework used to control the plant's performance.

3.1 Plant subsystems

Control of overall performance of the MDBR plant can be established through manipulation of decision variables of each of the individual sub-

systems. The plant schematic presented in Figure 3.1 illustrates that the main subsystems of the plant are:

- Solar Energy Collection System: Energy from the sun is harvested through solar panels. Solar energy is transferred to the batteries and the thermal storage system through their respective panels.
- Solar Energy Thermal Storage System: Part of the solar energy collected is transferred to the thermal storage tank. Energy is stored through the heat capacity and the change in temperature of the material.
- Membrane Distillation Bio-Reactor (MDBR): The recycling of waste water is facilitated by the presence of the MDBR. The purification process is aided by organic material and bio-degradation inside the MDBR.
- Heat Recovery System: Much of the heat supplied to the system will be rendered useless through losses unless it is recovered. Hence to increase efficiency, the system requires heat recovery. Heat recovery is effected through the usage of heat exchangers and heat pumps.

3.2 Plant operation

As the solar radiation increases at dawn, the solar collectors and the solar thermal storage system kick into action. These two subsystems working in conjunction help sustain the thermal and electrical load required to produce

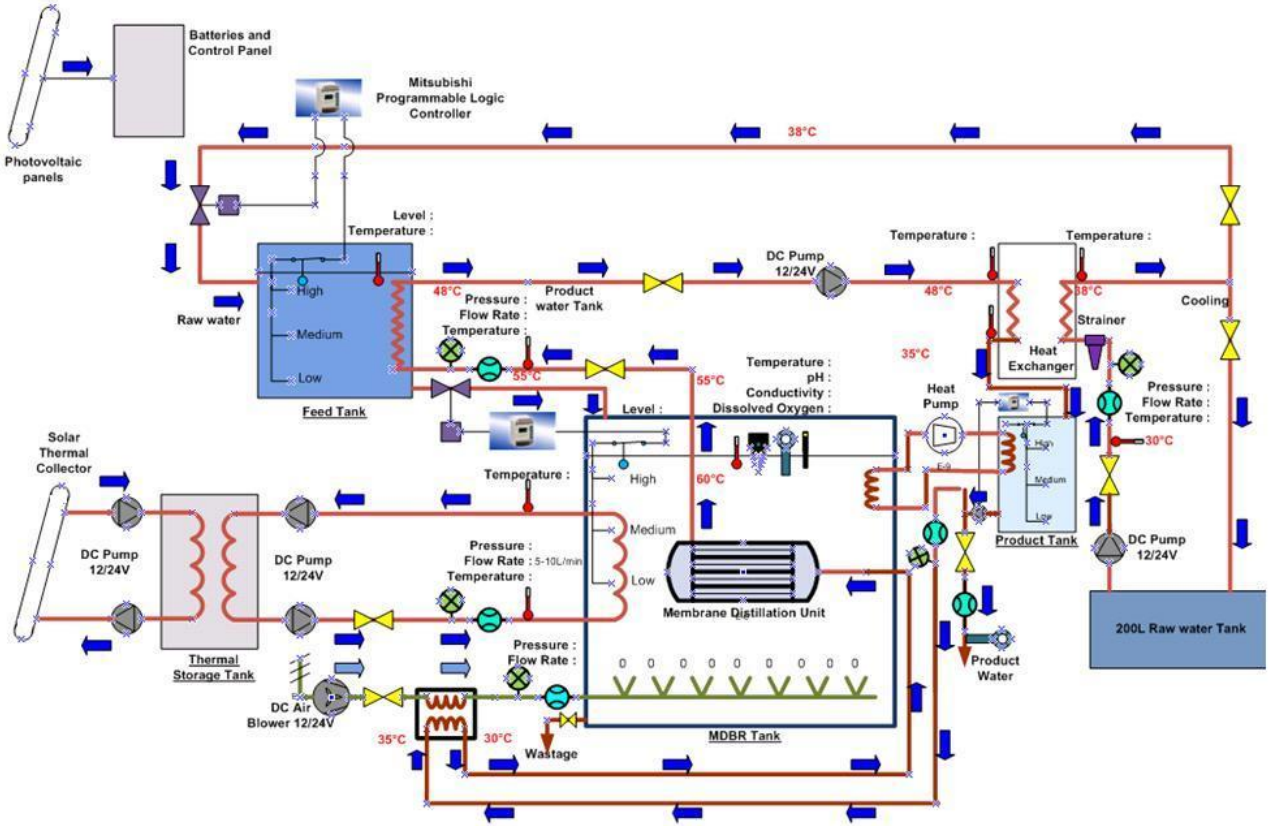

Figure 3.1: Plant Schematic[11]

clean water. The recycling of waste water is facilitated by the presence of the MDBR. The purification process is aided by organic material and biodegradation inside the MDBR. The waste water feed and the clean permeate streams move parallel to the membrane surface but in opposite directions inside the MDBR. The vapor pressure difference enables the water vapor to diffuse and/or convect across the membrane to the permeate side where it is condensed.

The feed and the permeate streams also come into contact with each other in the feed tank. The feed tank acts as a heat exchanger where energy is transferred back to the feed from the permeate. To ensure smooth operation, the feed and the permeate streams have to be returned to their original temperature before they enter the MDBR module. The thermal storage tank is used to heat the feed stream. Energy harnessed by the solar collectors is stored in the thermal storage tank before it can be utilized by the MDBR.

The permeate stream is allowed to pass through another heat exchanger to enhance energy recovery and further reduce its temperature. The temperature at which the permeate stream enters the MDBR is controlled through this unit. The flow rate of the cold stream is manipulated to control permeate temperature. The cooling liquid used for this purpose is pumped from the main raw water storage tank.

During stable operation, there is a build up of product water in the permeate stream. This build up is removed and stored in the product tank separately.

3.3 Plant modeling

In order to be incorporated into an optimization problem, the changes in output signals with respect to changes in input signals of plant need to be modelled. The models presented in this chapter are static, in other words, steady state. Such models have been used since it is assumed that the time scale at which the process dynamics occur is much smaller than the time scale at which the optimized control strategies are deployed and hence can be handled via standard regulatory layer control. This work focuses more on the optimization aspects than detailed modeling of the process and hence model uncertainties were not considered. Expressions which can be used to capture the general relation between the outputs and the inputs of the system are sufficient to determine viable optimal operating conditions.

3.3.1 Output flux

Output flux is the product of the membrane coefficient and the vapor pressure gradient between the feed and the permeate[1]. The driving force required to produce output flux is imposed by a temperature gradient between the feed and the permeate side[26]. The close resemblance between the temperature and vapor pressure profiles illustrated in Figure 3.2 indicates that the flux driving force (characterized by a temperature gradient) can be used as a proxy in place of the output flux (characterized by a vapor pressure gradient).

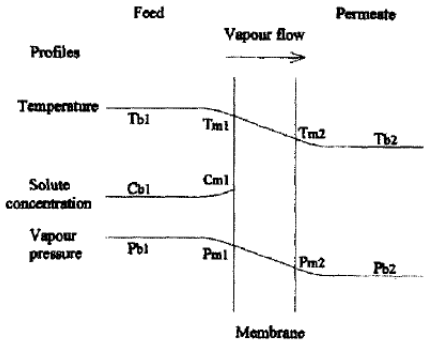

Figure 3.2: Temperature and vapor pressure profiles across the membrane cross section. (the horizontal axis is the position along the thickness of the membrane)[48]

An experiment was performed to verify the validity of the use of flux driving force as a proxy. The values of the temperatures on the feed and the permeate side were varied to observe the changes in output flux. Since the output flux is proportional to the driving force as shown in Fig. 3.3, the control system can manipulate the value of flux driving force instead of the output flux while determining the control strategy. The flux driving force, J, is difference between the MDBR temperature and the average temperature of re-circulation as shown by the following equation:

$$J = T_{mdbr} - 0.5(T_{out} + T_{in}) \tag{3.1}$$

where T_{mdbr}, T_{out} and T_{in}denote [3.1]the temperature inside the MDBR, at the outlet and inlet of the re-circulated liquid respectively.

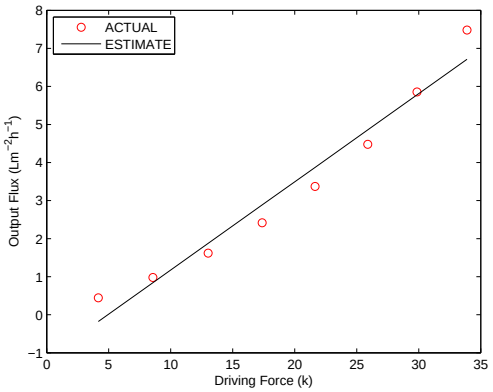

Figure 3.3: Model validation - Output flux

3.3.2 Power consumed

Power is consumed by the plant in two different forms: electrical and thermal. Electrical power, P_{load}, is divided amongst the circulation pump for the feed liquid, P_{feed}, circulation pump for the re-circulated liquid P_{circ} and the power supplied to the heat pump, P_{hp}.

$$P_{load} = P_{feed} + P_{circ} + P_{hp} \tag{3.2}$$

Since all the pumps used are centrifugal in nature, shaft power consumed is proportional to their respective flow rates F_{feed} and F_{circ} as shown by Fig. 3.4[49].

$$P_{load} = K_p F_{feed} + K_p F_{circ} + P_{hp} \tag{3.3}$$

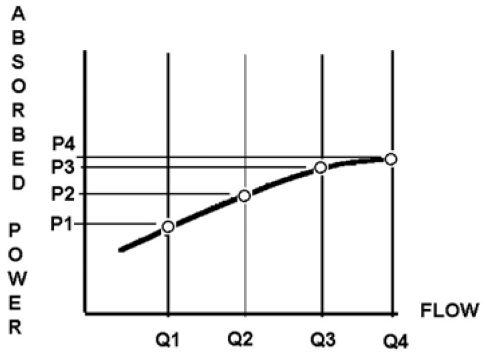

Figure 3.4: Model validation - Power-flow characteristics of typical centrifugal pump[49]

Main thermal power requirements considered are that of feed liquid , Q_{feed}, re-circulated liquid, Q_{circ} and MDBR tank loss, Q_{mdbr}. The heat recovered by the heat pump, Q_{hp}, should be assigned a negative sign in the expression for the overall thermal power consumed. Hence, the resulting expression can be represented as:

$$Q_{load} = Q_{feed} + Q_{circ} + Q_{mdbr} - Q_{hp} \tag{3.4}$$

When expanded, the above equation is of the form:

$$\begin{aligned} Q_{load} &= F_{feed}C_p(T_{mdbr} - T_{feed}) + F_{circ}C_p(T_{out} - T_{in}) \\ &\quad + hA(T_{mdbr} - T_{amb}) - P_{hp}CoP \end{aligned} \tag{3.5}$$

The constants $h, A, C_p$and CoP denote the heat transfer coefficient of the MDBR tank, the surface area of the MDBR tank, the specific heat

capacity of water and the coefficient of performance of the heat pump. The terms T_{feed} and T_{amb} correspond to the temperatures of the feed liquid and the ambient conditions.

3.3.3 Re-circulated liquid

The output flux depends upon the inlet and outlet temperatures of the re-circulation liquid. The inlet temperature is maintained constant through control of flow rate of cooling liquid in heat exchanger as shown by Abdelghani-Idrissi et al.[50]. The outlet temperature of re-circulated liquid can be determined by equating the thermal power consumed by re-circulation liquid to the product of surface area, heat transfer coefficient and logarithmic mean temperature difference (LMTD) of the MDBR tank[32] as follows:

$$\frac{hA\left[(T_{mdbr}-T_{out})-(T_{mdbr}-T_{in})\right]}{log\left(\frac{T_{mdbr}-T_{out}}{T_{mdbr}-T_{in}}\right)} = F_{circ}C_p(T_{out}-T_{in}) \tag{3.6}$$

which can be re-written as,

$$T_{out} = T_{mdbr} + e^{\frac{-hA}{C_p F_{circ}}}(T_{in}-T_{mdbr}) \tag{3.7}$$

An experiment was performed to verify the validity of the use of this relation also. It can be discerned from the above equation that the parameters which affect outlet temperature of re-circulated liquid are: inlet temperature of re-circulated liquid, flow rate of re-circulated liquid and MDBR temperature. Since the equipment available does not support changes in flow rate, the experiments only involved changes in inlet temperature of

re-circulated liquid and MDBR temperature. When flow rate is maintained constant, the relation reduces to:

$$T_{out} = T_{mdbr}(1 - e^{\frac{-hA}{C_p F_{circ}}}) + T_{in}(e^{\frac{-hA}{C_p F_{circ}}}) \tag{3.8}$$

where both coefficients are constant. Hence, the change in outlet temperature of re-circulated liquid is proportional to both the above mentioned parameters as seen in Fig 3.5. Since each graph only shows the variation of outlet temperature with respect to one parameter (either inlet or MDBR temperature), changes in the other parameter during collection of data can cause minor deviations from linearity. It can be observed from Figure 3.5 that the accuracy of the estimated relation has not been compromised due to the presence of such deviations.

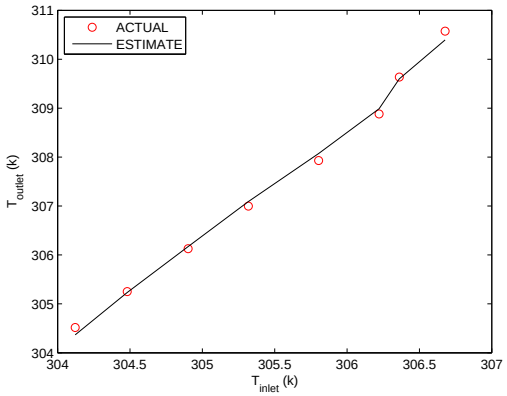

(a)

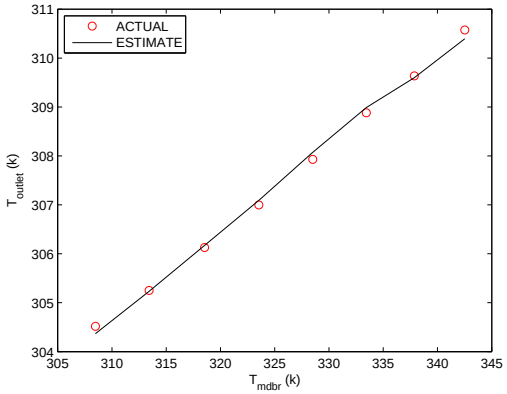

(b)

Figure 3.5: Model validation - Re-circulated liquid (a)Variation with respect to inlet temperature (b)Variation with respect to MDBR temperature

The references used for the plant equations mentioned here have been summarized in Table 3.1.

Table 3.1: Reference table for plant equations

Equation No.	Reference
3.1	[1, 26]
3.3	[51]
3.5	[51]
3.6	[32]

3.4 Block diagram description

The quantities in the equations discussed Section 3.3 have been presented in a block diagram in Figure 3.6 to enhance comprehension on how the entire solar powered MDBR plant works. Let us analyze how variation in different quantities is the plant are interconnected or related to each other. From equations 3.1 to 3.7 we know that,

$$\begin{aligned} J &= T_{mdbr} - 0.5T_{out} - 0.5T_{in} \\ P_{load} &= K_p F_{feed} + K_p F_{circ} + P_{hp} \\ Q_{load} &= F_{feed} C_p (T_{mdbr} - T_{feed}) + F_{circ} C_p (T_{out} - T_{in}) \\ &\quad + hA(T_{mdbr} - T_{amb}) - P_{hp} CoP \\ T_{out} &= T_{mdbr} + e^{\frac{-hA}{C_p F_{circ}}} (T_{in} - T_{mdbr}) \end{aligned}$$

where each term in the above equations can be associated with specific subsystems. A more detailed list of system parameters has been presented in Table 3.2 on page 50. These parameters will later be used during simulation in Section 4.5.1 on page 64.

Since the quantities associated with the MDBR plant are interconnected with each other, it is useful to examine how each quantity is related to the

others. Output flux J from equation 3.1 is dependent on the values of the temperatures inside the MDBR T_{mdbr}, outlet temperature of recirculated liquid T_{out} and inlet temperature of recirculated liquid T_{in}. It is also known from equation 3.7 that the outlet temperature of recirculated liquid T_{out} is related to the temperatures T_{mdbr}, T_{in} and the flow rate F_{circ}. Hence, if the temperature inside the MDBR tank increases, the value of the output flux increases. And if either the temperature of the inlet or the outlet temperature increases then the temperature gradient decreases, causing the flux to decrease. The relation which is not as easy to recognize is the one between flow rate of recirculation F_{circ} and the output flux J. As F_{circ} increases, the amount of time the recirculated liquid spends inside the MDBR tank decreases. This causes the temperature of the outlet to decrease since it is not getting warm from the heat in the MDBR tank. As the value of T_{out} decreases the temperature gradient between the MDBR and recirculated liquid increases leading to an increase in output flux. It is obvious that an increase in T_{mdbr} or an increase in F_{circ} will lead to an increase in Q_{load} and P_{load} respectively. So more flux requires more thermal and electrical consumption. The different elements of consumption have been specified in equations 3.5 and 3.3. The electrical and thermal power consumed increases when quantities such as F_{feed}, F_{circ} and T_{mdbr} increase. Whereas, an increase in T_{amb}, T_{feed} and T_{in} leads to a decrease in Q_{load}. Hence, different quantities or "knobs" have different effects on the operation of the MDBR plant.

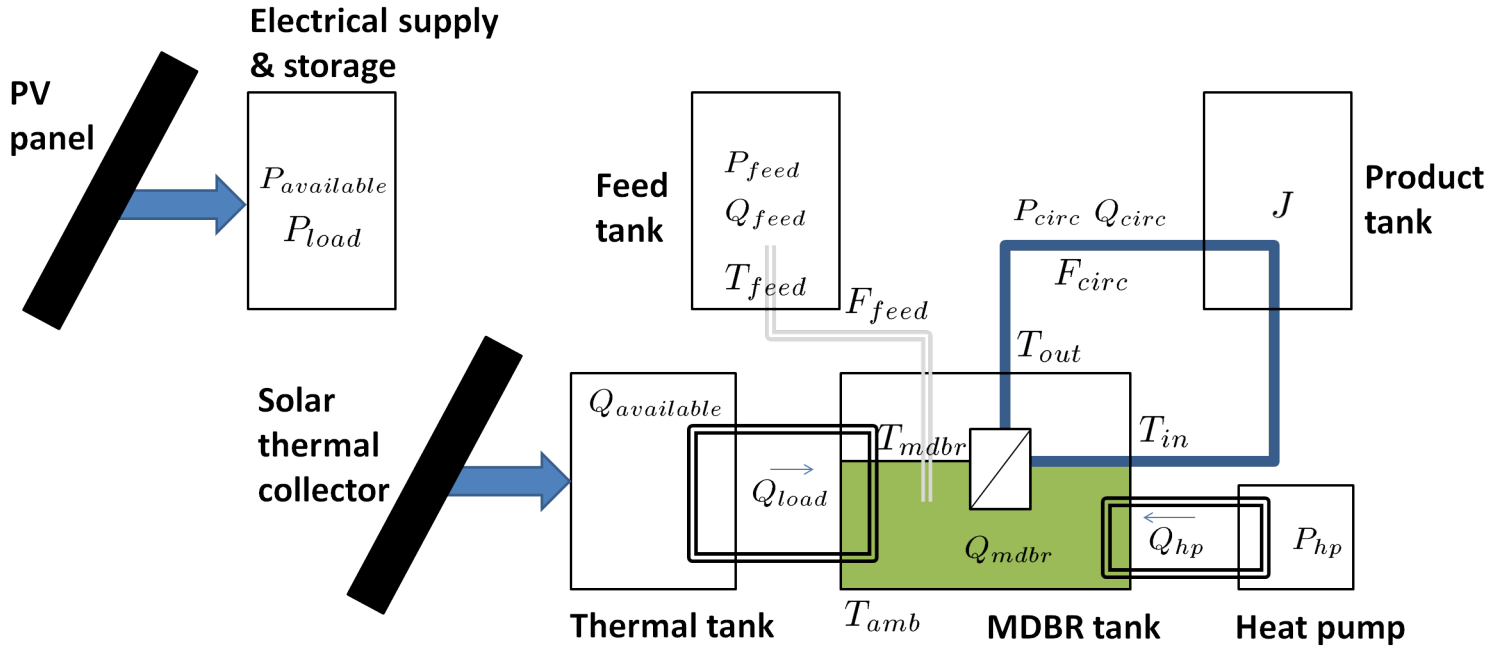

Figure 3.6: Block diagram description

Table 3.2: MDBR plant parameters

Symbol	Value
C_p	$4.2 \times 10^3\ kJm^{-3}k^{-1}$
h	$0.03\ kWm^{-2}k^{-1}$
A	$2\ m^2$
CoP	3
T_{in}	$305\ K$
T_{feed}	$303\ K$
T_{amb}	$303\ K$
$F^{max}_{(circ,feed)}$	$10\ lmin^{-1}$
$F^{min}_{(circ,feed)}$	$3\ lmin^{-1}$
P^{max}_{hp}	$2\ kW$
P^{min}_{hp}	$0\ kW$
T^{max}_{mdbr}	$353\ K$
T^{min}_{mdbr}	$328\ K$
$T_{sustenance}$	$318\ K$

3.5 Control framework

3.5.1 Objectives motivating control

The three main factors that have been considered for the solar powered MDBR plant are:

- Safety: The control system must ensure that the plant remains stable at all times. None of the operational constraints must be violated under any circumstances. In effect this means that the control system should take into account the limits of the components in the plant. The temperature range required for the MDBR micro-organisms to survive and the component constraints associated with the circulation and heat pumps need to be considered.

- Self-sustaining operation: The plant is designed to derive its primary source of energy from solar radiation. It has to function independently without requiring external sources of power once it has been commissioned. External intervention or support from auxiliary equipment should be required only in dire circumstances. This requires the plant to reduce production and accumulate back up reserves in some situations even if plenty of solar radiation is available. This will allow the plant to possess sufficient reserves to ensure that the minimum temperature required for micro-organisms can be sustained at all times without any external assistance.

- Maximizing output produced from available energy: This objective is related to the economic feasibility of the plant. The production levels have to justify the high capital costs of the infrastructure required. Hence, the operating conditions must ensure that the plant produces the maximum amount of output that is physically possible while making use of the available solar reserves.

3.5.2 Control configuration

The disparate nature of system objectives increases the complexity of the control scheme. A global controller capable of handling all control functions is not suitable for such applications due to its associated drawbacks drawbacks: low fault tolerance, lack of structural flexibility and high computational costs. Hence the hierarchical framework described in Section 2.4 is used as shown in Figure 3.7. The functions of the different layers are

described below:

- Scheduling layer: This layer decides how to cope with changes in weather conditions several days in advance. It manages system reserves based on information available from the solar radiation prediction system to ensure continuous operation. Hence, it is closely related to self sustaining operation.

- Supervisory layer: This layer determines how the system will handle variation in solar radiation from dawn to dusk. Depending on the solar radiation levels, the supervisory layer will either manipulate production rate along with power consumed or cease production to focus on survival of micro-organisms. Hence, it is closely related to safety and maximizing the output produced from the available energy.

- Regulatory layer: This layer minimizes set point deviations due to internal and external disturbances.

The time constants or time interval between control signals for each layer are as follows: four hours for the scheduling layer, one hour for the supervisory layer and hundred milliseconds for the regulatory layer. This thesis will not concern itself with the regulatory layer. It can be implemented through standard process control techniques such as PID control which have been extensively studied and documented [52]. The design and evaluation of the supervisory and scheduling layers are discussed in detail in the subsequent chapters.

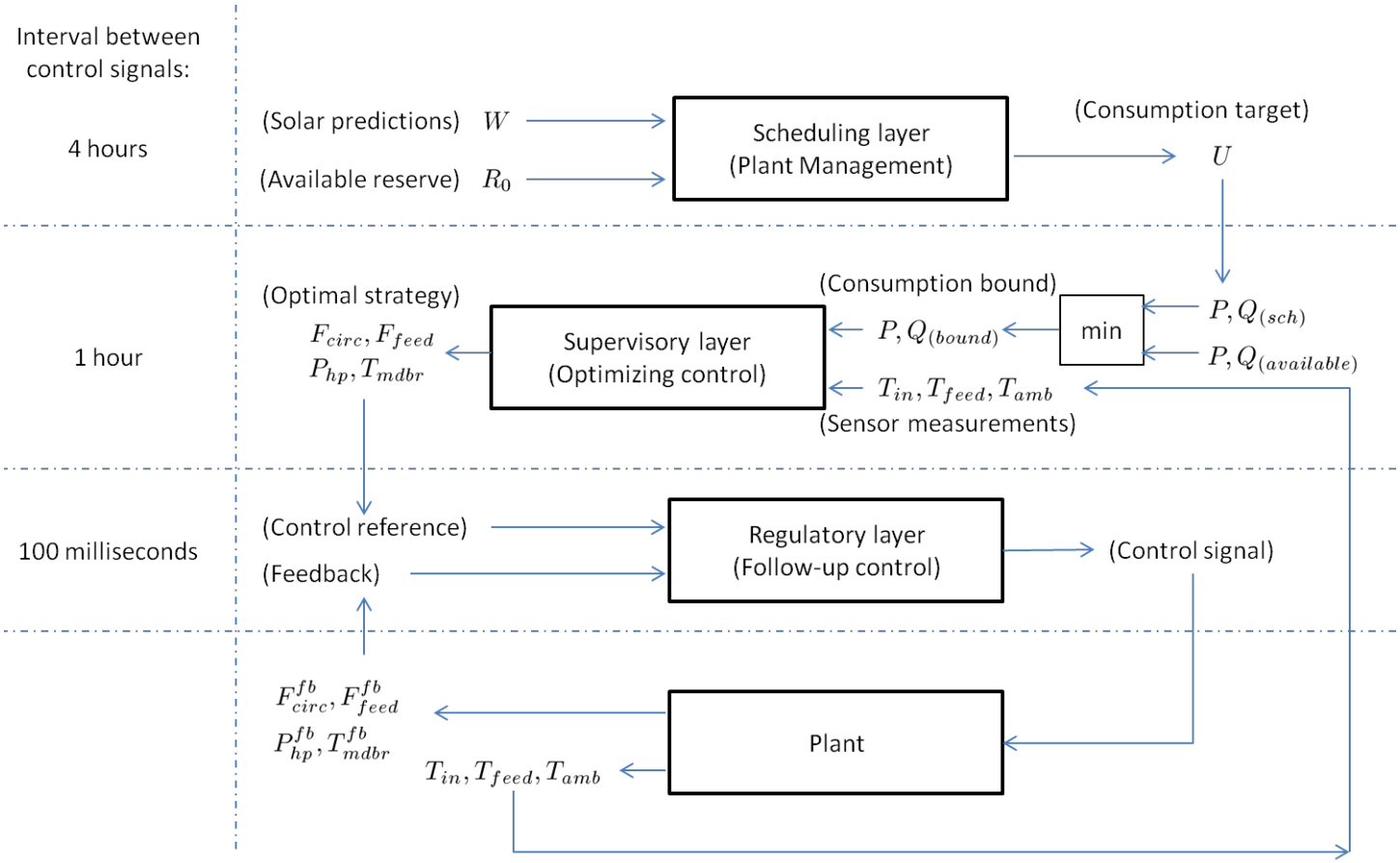

Figure 3.7: MDBR control framework

3.5.3 Measured and manipulated variables

The selection of measured and manipulated variables shown in Figure 3.7 was done through the analysis of cause and effect relationships embedded into the equations that describe the plant. The main knobs or manipulated parameters for the control framework are: the bounds on consumption $P, Q_{(bound)}$ from the scheduling layer and the optimal values of $F_{feed}, F_{circ}, P_{hp}$ and T_{mdbr} from the supervisory layer. As for the regulatory layer, it assumes the values of $F_{feed}, F_{circ}, P_{hp}$ and T_{mdbr} from the supervisory layer as control references and collects feedback for the same to minimize set point deviations. Other variables which need to be measured are T_{in}, T_{feed} and T_{amb}(for the supervisory layer). It should be noted that this work assumes knowledge of certain quantities for its operation. These are, solar predictions over a planning horizon of five days W, current or available reserve for the scheduling layer R_0 and the current or available reserve for the supervisory layer $P, Q_{(available)}$.

3.6 Chapter summary

This chapter provides an overview of different facets of the solar powered MDBR plant. It begins with discussions of top level subsystems that constitute the MDBR plant. Such a top level understanding makes way for an explanation of plant operation and the mathematical relations that are associated with the plant. These mathematical relations can be better appreciated through use of the block diagram description presented. Based on the plant description and control requirements a suitable control framework

has been constructed to serve the purposes of plant-wide control.

Chapter 4

Design and Evaluation of the Supervisory Layer

Real time optimization and mode selection are the two main functions of the supervisory control layer. Data acquired through assessment of available energy reserves and possible loads required by the plant guide the optimization and mode selection process. The optimization problem in this layer focuses on the amount of clean water produced and the power consumed while adhering to the constraints imposed by the plant. In Section 4.4, the different ways in which such an optimization problem can be formulated is discussed. Since these problems are inherently non-convex, relaxations and approximations are required to obtain a convex optimization problem. These alterations are discussed in Sections 4.5.2 and 4.5.3. Section 4.6 shows simulation results that demonstrate the performance of the supervisory layer. The results obtained from simulations are then used to compare the performance of the different formulations and choose the

best alternative.

4.1 Objective

The main objective of the supervisory layer is to make the best use of the available power. It aims to manipulate the operating conditions such that the plant is able to find the right balance between production rate and power consumed.

The supervisory layer should be able to prioritize its objectives according to the varying environmental conditions. It has to be able to ascertain which objectives require attention during different parts of the day. For this purpose, it needs to operate in different modes as explained in the next section.

4.2 Modes of operation

The current mode of operation depends on the available reserves and solar radiation levels. When the reserves available are sufficient to support the load required by the MDBR plant to produce clean water, it will operate in production mode. If this condition cannot be satisfied, the system will operate in sustenance mode.

4.2.1 Production mode

Variation in solar radiation results in a variation in available solar reserves. To cope with these variations, real time optimization is required. The main

objectives that need to be taken into consideration in this mode of operation are minimization of power consumed and maximization of output produced.

4.2.2 Sustenance mode

When available solar radiation is weak, the system ceases to produce output. Re-circulation is not required since it is used mainly to transfer the build up of clean water from the permeate stream to the product tank. The objective here is to maintain the conditions required for survival of micro-organisms inside the MDBR and minimize the power consumed while doing so. Real time optimization is not required for this purpose and can be achieved through operation of the regulatory layer itself.

Remark 1

The system switches between modes when the available power is above the threshold value. Since circulation pumps will be functional in both modes of operation, the plant is designed to support the power required by the pumps at all times.

Remark 2

The main factor which determines mode of operation is the minimum thermal power required to produce clean water. If the available power is above this value, the plant will operate in production mode. This minimum thermal power or threshold value is calculated from the solution of an optimization problem discussed in later in this chapter.

4.3 Optimization problem

The supervisory layer optimization problem will attempt to minimize a certain objective function $c(x, u)$ while satisfying a set of constraints $h(x, u) \leq 0$. The symbols x and u represent the state variables and the manipulated variables respectively. Hence the general optimization takes the form:

$$\begin{aligned} \underset{U}{\text{minimize}} \quad & c(X, U) \\ \text{subject to} \quad & h(X, U) \leq 0 \end{aligned} \tag{4.1}$$

where

$$X = \begin{bmatrix} T_{amb} \\ T_{feed} \\ T_{in} \end{bmatrix} \quad \text{and} \quad U = \begin{bmatrix} F_{circ} \\ F_{feed} \\ P_{hp} \\ T_{mdbr} \end{bmatrix}$$

The manipulated variables F_{circ} and F_{feed} represent the flow rate of the re-circulated liquid and the feed liquid. The other manipulated variables, P_{hp} and T_{mdbr} represent the power supplied to the heat pump and the temperature inside the MDBR. The state variables or measured variables T_{amb}, T_{feed} and T_{in} represent the temperatures of the ambient surroundings, the feed liquid and the inlet of the re-circulated liquid. The real-time optimization is based on the temperatures as real-time measurements and the knowledge of the available power for (only) the current period from the solar radiation data.

4.4 Proposed approaches to plant-wide control and optimization

There exists more than one way in which the main design objectives can be addressed. This thesis considers three main variations which have different advantages and disadvantages as discussed by the following sections.

4.4.1 Threshold calculation

This computation is carried out determine the minimum power level required to produce clean water. The optimization problem is formulated such that the objective function minimizes the power consumed while satisfying the constraints imposed by the components to operate in production mode.

$$\begin{aligned} \underset{U}{\text{minimize}} \quad & Q_{load} + P_{load} \\ \text{subject to} \quad & \underline{U} \leq U \leq \overline{U} \end{aligned}$$

where Q_{load} and P_{load} represent the thermal and electrical power consumed. The component operational limits in production mode are represented by $\underline{U}$ and $\overline{U}$. This problem is solved at the design stage to select a threshold value according to the sizing and specifications of the equipment available.

4.4.2 Weighted Sum Optimization (WSO)

Common practice in multiple objective optimization involves the usage of a weighted sum of the different objectives. The individual weights are subject

to the requirement of the designer. Such approaches focus on determining a single optimal operating point and aim to maintain those conditions irrespective of changes in external factors. The popularity of these approaches can be attributed to their simplicity. But, when applied to the supervisory layer, they do not guarantee that the solution will simultaneously maximize the output produced and the power consumed. They only guarantee that the solution optimizes a relative weighted sum of the objectives. The weighted sum approach is suitable for the the determination of a stationary operating point which implicitly assumes that the available energy will be sufficient to support the determined operating point at all times. Since, this is not the case in practice, a better approach is required. The WSO approach results in an optimization problem of the form:

$$\begin{aligned} \underset{u}{\text{minimize}} \quad & -\delta_1 J + \delta_2 (Q_{load} + P_{load}) \\ \text{subject to} \quad & \underline{U} \leq U \leq \overline{U} \end{aligned}$$

4.4.3 Repeated Optimization (RO)

Another strategy could be to remove the output flux from the objective function and include it as a constraint. Thus, the optimization problem will minimize power consumed while forcing the output flux to take different values between its nominal minimum and maximum bounds. Multiple optimization problems will be solved with different values of flux as a constraint. Hence this will result in multiple operating points which form a set of possible options on how to operate the plant. During operation, the combination which is closest to the current reserve level is chosen as the

control law. The resulting optimization problem takes the form:

$$\begin{aligned} \underset{U}{\text{minimize}} \quad & Q_{load} + P_{load} \\ \text{subject to} \quad & J \geq J_i \in [J_{min}, J_{max}] \\ & \underline{U} \leq U \leq \overline{U} \end{aligned}$$

The main drawback of this approach is the high computational load it imposes on the system. Numerous optimization problems will have to be solved before the operating point can be determined. Such computational loads are justified if they are used offline to determine different sets of optimal operating points corresponding to different conditions.

4.4.4 Power Constrained Optimization (PCO)

This strategy involves solving a different optimization problem each time the operating points have to be determined. Since it has to be solved online, it does not have the luxury of attempting to solve numerous optimization problems before the desired operating points are determined. Hence, it has to succinctly capture all of the plant's requirements in one optimization problem. Maximizing the output flux while imposing bounds on the power consumed will allow the plant to address both design objective through the use of a single optimization problem. The resulting optimization problem takes the form:

$$\begin{aligned} \underset{U}{\text{maximize}} \quad & J \\ \text{subject to} \quad & Q_{load} \leq Q_{bound} \\ & P_{load} \leq P_{bound} \\ & \underline{U} \leq U \leq \overline{U} \end{aligned}$$

For the sake of comprehension, these bounds on power consumed will correspond to the available reserve levels in this discussion. During the course of the following chapters, these bounds will depend on other factors also.

4.5 Implementation

To compare the performance of approaches presented above, they have to be incorporated into convex optimization problems and tested with simulations of the MDBR plant. There are certain issues which need to be resolved before this can be done, namely, simulation details, non-convexity and selection of weights in the WSO approach. Since some relations that are common to all of the approaches considered are non-convex, changes are required to solve them using convex optimization are described. Subsequently, this section discusses the justification required for selection of a suitable operating point after examining different values of the weights (δ_1 and δ_2) in the WSO approach.

4.5.1 Model simulation

Before proceeding to the simulation details, let us state the assumptions being made about the MDBR plant's operation at each sampling period:

- The temperature of feed liquid T_{feed}, ambient temperature T_{amb} are known from measurements and remain constant.
- The heat recovery system maintains the inlet temperature of the recirculation liquid T_{in} constant at the measured value.
- The plant is designed to support the power required by the circulation pumps at all times.
- The available reserve or the maximum power that can be consumed by the plant during the current sampling period is known.
- The main mode of control for the thermal storage tank will be associated with regulatory control for the temperature inside the MDBR tank, T_{mdbr}. By virtue of the assumption above, the optimization problem will not calculate a value of T_{mdbr} that is not physically viable or is beyond the limits of the available reserve at the current sampling period. Since the regulatory layer is assumed to be fully functional and capable of enforcing the reference values determined by the optimization problem, plant operation will proceed smoothly.

The cost functions are dependent on the values of the manipulated variables. From equations 3.1 to 3.5 we know that,

$$
\begin{aligned}
J &= T_{mdbr} - 0.5T_{out} - 0.5T_{in} \\
P_{load} &= K_p F_{feed} + K_p F_{circ} + P_{hp} \\
Q_{load} &= F_{feed} C_p (T_{mdbr} - T_{feed}) + F_{circ} C_p (T_{out} - T_{in}) \\
&\quad + hA(T_{mdbr} - T_{amb}) - P_{hp} CoP
\end{aligned}
$$

where all parameters except T_{out} are known. They are either measurements such as T_{in}, T_{feed} and T_{amb} or constants such as C_p, h, A and CoP or values known from the optimization solution for the manipulated variable such as $F_{circ}, F_{feed}, P_{hp}$ and T_{mdbr}. From equation 3.7 we know that the link between the cost functions and the model of the plant is,

$$T_{out} = T_{mdbr} + e^{\frac{-hA}{C_p F_{circ}}}(T_{in} - T_{mdbr})$$

Now, since the value of T_{out} can be calculated from the information already known, this constitutes an analytical solution to the model of the process. The procedure in the closed loop simulation block diagram from Figure 4.1 on the following page has been implemented in Matlab using the parameters specified in Table 4.1. Upon careful examination, one will notice that the model is not explicitly represented as an equality constraint in the proposed approaches in Section 4.4 but rather included in the cost functions and the inequality constraints in the thesis. This has been done since the model of the process can be analytically solved. But this analytical solution is not convex and hence cannot be readily incorporated into the convex optimization framework. The following section provides more details pertaining to this issue.

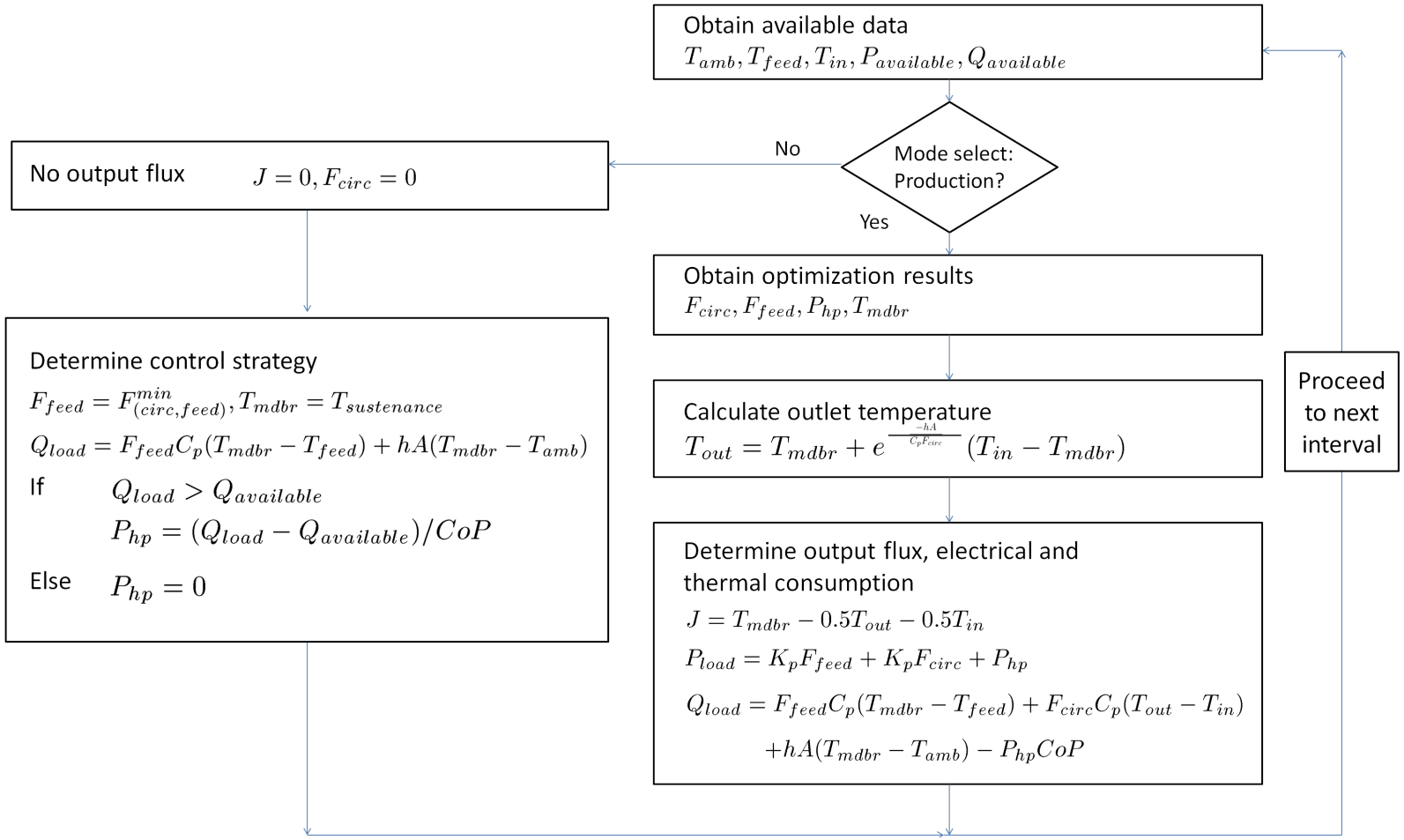

Figure 4.1: Simulation block diagram - Supervisory Layer

Table 4.1: Supervisory layer parameters

Symbol	Value
C_p	$4.2 \times 10^3\ kJm^{-3}k^{-1}$
h	$0.03\ kWm^{-2}k^{-1}$
A	$2\ m^2$
CoP	3
T_{in}	$305\ K$
T_{feed}	$303\ K$
T_{amb}	$303\ K$
$F^{max}_{(circ,feed)}$	$10\ lmin^{-1}$
$F^{min}_{(circ,feed)}$	$3\ lmin^{-1}$
P^{max}_{hp}	$2\ kW$
P^{min}_{hp}	$0\ kW$
T^{max}_{mdbr}	$353\ K$
T^{min}_{mdbr}	$328\ K$
$T_{sustenance}$	$318\ K$
Time interval between change in control strategy (sampling period)	1 hour

4.5.2 Non-convex compatibility issues

The mathematical expressions that govern different quantities have already been presented in Section 3.3. When written in terms of the control variables u, equations 3.1 to 3.5 take the following form:

$$J = u_4 - c_1 t_{out}(u_1, u_4) - c_2 \tag{4.2}$$

$$P_{load} = c_3 u_1 + c_4 u_2 + u_3 \tag{4.3}$$

$$\begin{aligned} Q_{load} &= c_5 u_1 t_{out}(u_1, u_4) - c_6 u_1 + c_7 u_2 - c_8 u_2 u_4 \\ &\quad + c_9 u_4 - c_{10} u_3 - c_{11} \end{aligned} \tag{4.4}$$

where $c_i > 0 \, \forall i$ and the function $t_{out}(u_1, u_4)$ representing outlet temperature of re-circulated liquid is described by:

$$t_{out}(u_1, u_4) = u_4 + e^{\frac{-c_{12}}{u_1}}(2c_2 - u_4) \tag{4.5}$$

the terms J, P_{load} and Q_{load} represent the flux driving force, electrical power consumed and the thermal power consumed respectively.

The expressions that need to be used in the optimization problem are non-linear and non-convex in their original form. Hence, its solution cannot be determined through convex optimization algorithms. Some equations and functions need to be modified before they can be incorporated into the optimization problem. These modifications are important for the formulation of a convex optimization problem. When all functions and constraints are convex, the necessary and sufficient conditions to determine the global minimum are given by Karush-Kuhn-Tucker (KKT) conditions[40]. CVX[53] is the software package used to solve convex optimization problems in this thesis. This package requires the problem to be compatible with the disciplined convex programming rule set. Terms which do not comply with the above criteria are: functions that contain $t_{out}(u_1, u_4)$ in equations 4.2 and 4.4 and the bi-linear term $c_8 u_2 u_4$ in equation 4.4. The Hessian cannot be proved to be positive semi-definite in these cases. Hence, they cannot be considered convex.

4.5.3 Obtaining convex problems

This thesis considers two methods to obtain convex problems: sequential convex programming and convex relaxations. These methods are used to formulate problems that closely resemble the original supervisory layer optimization problem and can be solved through disciplined convex programming.

4.5.3.1 Sequential convex programming

In general solutions of non-convex problems have to be a trade off between computation time and optimality. Sequential convex programming (SCP) attempts to use a sequence of convex portions of the non-convex problem such that the final solution is near the global optimal value. SCP is usually used with a problem of the form:

$$\begin{aligned} \underset{x}{\text{minimize}} \quad & f_0(x) \\ \text{subject to} \quad & f_i(x) \leq 0 \quad i = 1, \ldots, m \\ & h_j(x) = 0 \quad j = 1, \ldots, p \end{aligned}$$

where the functions $f_i, i = 0, .., m$ are possibly non-convex and the functions $h_j, j = 1, .., p$ are possibly non-affine. SCP will generate an estimate of the solution $x^{(k)}$ over a convex trust region $T^{(k)}$ with a trust radius $\rho^{(k)}$. Trust regions are usually made up of bounding boxes around specific points. The solution $x^{(k)}$ is determined by using convex approximations $\hat{f}_i$ of f_i over trust region $T^{(k)}$ and an affine approximation $\hat{h_j}$ of h_j over trust region $T^{(k)}$. If the change in objective function, inequality and equality violations

are favorable, the size of the trust region around the given point is increased and the SCP process is repeated.

It is easy to see that the results of SCP are heavily influenced by the starting point selected. As a trust region only considers a specific portion of the total range of the control variables, the resulting problem can and often does become infeasible as shown in Table 4.2 depending on the starting point chosen. Hence, SCP is not reliable and not suitable for solving the supervisory layer optimization problem.

Table 4.2: Infeasibility issues in SCP

(a) SCP used in Repeated Optimization (RO) when $J_i = 40K$

Starting Point				Feasibility
$F_{circ}(m^3/s)$	$F_{feed}(m^3/s)$	P_{hp}(kW)	T_{mdbr}(K)	
0.0001667	3.33E-05	0	346.0258709	Feasible
6.09E-05	0.000106416	1.638134017	340.3283548	Infeasible
6.00E-05	0.00012852	0.678105484	344.1024438	Infeasible
7.64E-05	0.00012506	1.902843501	332.5000529	Infeasible
3.40E-05	0.000150581	1.385888468	331.2358088	Infeasible

(b) SCP used in Power Constrainted Optimization (PCO) when $Q_{bound} = 10kW$ and $P_{bound} = 0.16kW$

Starting Point				Feasibility
$F_{circ}(m^3/s)$	$F_{feed}(m^3/s)$	P_{hp}(kW)	T_{mdbr}(K)	
6.02E-05	0.000116472	1.098759757	341.871499	Feasible
0.000166696	5.47E-05	0.00093561	341.9992493	Infeasible
0.000122402	9.06E-05	1.885959289	342.1035037	Infeasible
4.37E-05	8.80E-05	0.536907527	348.3876751	Infeasible
0.000118057	1.62E-04	1.7487114	350.526656	Infeasible

4.5.3.2 Convex relaxations

Focussing on tighter convex relaxations of the non-convex expressions in the entire control envelope will help mitigate the issues faced by SCP. These convex relaxations are used replace their non-convex counterparts, giving rise to a convex optimization problem whose solution is close to the solution of the original problem. The optimization problem considered is of the form:

$$\begin{aligned} \underset{x}{\text{minimize}} \quad & f_0^r(x) \\ \text{subject to} \quad & f_i^r(x) \leq 0 \quad i = 1, \ldots, m \\ & h_j^r(x) = 0 \quad j = 1, \ldots, p \end{aligned}$$

The functions $f_i^r \forall i = 0, \ldots, m$ and $h_j^r \forall j = 1, \ldots, p$ are the convex relaxations used to replace the original functions. inequality and equality constraint functions respectively. One option that readily comes to mind is a linear relaxation. Linear programs (LPs) have been studied at length over the years and LP solvers are considered to be a mature technology whose associated computation times are small enough to be used in real time applications. Linear Programs can be easily solved using existing interior point algorithms. Hence the functions from equations 4.2 and 4.4 will be linear relations of the form:

$$\begin{aligned} c_1^T U + d_1 &= J \\ c_2^T U + d_2 &= Q_{load} \end{aligned}$$

where

$$
\begin{aligned}
c_1 &= \begin{bmatrix} 0.1874E05 \\ 0 \\ 0 \\ 0.9391 \end{bmatrix} \\
c_2 &= \begin{bmatrix} 0.0139 \text{ E } 05 \\ 1.60934 \text{ E } 05 \\ -3 \\ 0.5854 \end{bmatrix} \\
d_1 &= \begin{bmatrix} 16.6824 \end{bmatrix} \\
d_2 &= \begin{bmatrix} -198.6436 \end{bmatrix}
\end{aligned}
$$

These relaxations must also satisfy the constraints present in the proposed approaches, namely,

from RO (Section 4.4.3):

$$J \geq J_i \in [J_{min}, J_{max}]$$

and PCO (Section 4.4.4):

$$Q_{load} \leq Q_{bound}$$

otherwise the results obtained through optimization will violate the actual constraints. To this end, three dimensional plots of the non convex terms and the relaxations have been considered in Figure 4.2. One should notice that the camera angle is from the bottom in Figure 4.2(a) and that the

estimate (in black) is always greater than the actual value of J (in green). In Figures 4.2(b) and 4.2(c), the camera angle is from the top in order to show that the estimate (in in black) is always lower than the actual value (in green). It is also essential that the the relaxations provide results that are close to the optimum. In other words, they must closely resemble the original functions as seen in Figure 4.2, otherwise the true optimum will be missed.

As long as the relaxations used resemble the original relations satisfactorily, convex relaxations are superior to sequential convex programs. Convex relaxations can handle all of the expressions given above and do not present infeasibility issues.

The true test for these relaxations lies in their ability to produce viable optimal solutions when used in conjunction with the actual relations during simulation as demonstrated in Section 4.6. Now that a method to obtain convex problems has been established, one can proceed to analyzing different approaches to find global optimal solutions.

4.5.4 Selection of weights for WSO

It is not difficult to observe that the operating points determined through the WSO approach from Section 4.4.2 are dependent on the values of δ_1 and δ_2. To examine their influence on the optimal solutions, the value of δ_2 was varied while keeping $\delta_1$constant ($\delta_1 = 1$) . Table 4.3 shows that the process results in only two distinct operating points. For the sake of this discussion, the operating point in the top half of Table 4.3 will be referred

to as P1 and the other will be referred to as P2. If WSO were to be used, one of these two operating points has to be chosen. This choice becomes straight forward when one pays attention to a subtle nuance mentioned in Section 3.5. The hierarchical framework assumes that the regulatory layer will be able to enforce the set points determined by the supervisory layer at all times without requiring any external assistance. This is possible only if the available reserves are sufficient to sustain the load specified by the supervisory layer operating point. The load required by P2 corresponds to the minimum value required to operate in production mode. By virtue of the mode selection process in the supervisory layer, the solar thermal reserves will always be sufficient for the regulatory layer to enforce this set point. Since the same does not apply to P1, P2 is the operating point selected through WSO.

The fact that WSO results in only two distinct operating points is surprising and warrants further analysis. Such a shift in the operating point can be explained in terms of the shift in importance of the physical phenomena associated with the different weights. In other words, the weight associated with the respective physical quantity (flux driving force for $\delta_1$and power consumption for δ_2) influences the value of the objective function and hence the value of the solution of the optimization problem. The change in operating point represents the shift in dominance of one physical quantity over the other as there is a shift in weights.

Table 4.3: Supervisory layer - Weighted sum operating points

δ_1	δ_2	J (K)	$Q_{load} + P_{load}$ (kW)
1	1.00	46.1268	17.2918
1	1.17	46.1268	17.2918
1	1.33	46.1268	17.2918
1	1.40	46.1268	17.2918
1	1.44	46.1268	17.2918
1	1.49	46.1268	17.2918
1	1.50	46.1268	17.2918
1	1.52	46.1268	17.2918
1	1.53	46.1268	17.2918
1	1.54	46.1268	17.2918
1	1.57	46.1268	17.2918
1	1.58	46.1268	17.2918
1	1.59	46.1268	17.2918
	Operating	Point	Shift
1	1.61	22.1024	8.6706
1	1.62	22.1024	8.6706
1	1.63	22.1024	8.6706
1	1.66	22.1024	8.6706
1	1.67	22.1024	8.6706
1	1.67	22.1024	8.6706
1	1.68	22.1024	8.6706
1	1.70	22.1024	8.6706
1	1.71	22.1024	8.6706
1	1.76	22.1024	8.6706
1	1.80	22.1024	8.6706
1	1.83	22.1024	8.6706
1	2.00	22.1024	8.6706

4.6 Results and discussion

Plant-wide simulations were conducted using the relations described in Section 3.3. The different formulations: WSO, RO and PCO were pitted against each other. The three generic solar profiles used to analyze their performances:

- Typical solar profile: Solar radiation peaks at noon and gradually decreases on either side
- Intermittent solar profile: It consists of periods of sunshine interrupted by overcast conditions at noon
- Dark profile: It is characterized by a brief period of sunshine followed by overcast conditions throughout

The available power curves were obtained by proportionally scaling the value of solar radiation. They were obtained from the NREL Solar Radiation Research Laboratory (SRRL) Baseline Measurement System (BMS) data archive at http://www.nrel.gov/midc/srrl_BMS and the National Solar Radiation Data Base TMY3 data sets available at http://rredc.nrel.gov/. These solar profiles were chosen such that they are representative of the most common circumstances the plant is likely to encounter.

4.6.1 Case I: Typical solar profile

Figure 4.3 illustrates how the supervisory layer handles a generous supply of solar radiation. As the day progresses from dawn, the available power exceeds the required threshold. The system now realizes that production of output can commence. Hence, it switches to production mode as shown in Figure 4.3(b). As the solar radiation increases, the available power increases. Hence, the control strategy is manipulated accordingly. The amount of output produced and power consumed increases with an increase in available power as seen in Figure4.3(b) and 4.3(c). It can also be

seen from Figure 4.3(d) that the temperature inside the MDBR (T_{mdbr}) has a strong link with the output produced and power consumed. As long as the solar radiation is adequate to operate in production mode, the system does not need to expend electrical power through the heat pump to increase output flux as shown by Figure 4.3(e). One can understand from Figure 4.3(f) that the optimization problem generally selects the maximum value of flow rate for the re-circulated liquid. This is a consequence of its relation to the output flux as seen in Section 3.3.3. The optimization problem attempts to increase output flux by increasing flow rate of the re-circulation loop. The feed liquid on the other hand is assigned minimum flow rate so as to minimize the thermal and electrical power consumed as shown in Figure 4.3(g).

The differences between the formulations lie in how the control strategy is manipulated. The variation of flux driving force (J) and power consumed ($Q_{load} + P_{load}$) closely resembles the variation in solar radiation in the PCO approach as seen in Figures 4.3(b) and 4.3(c). In contrast, the RO approach gives rise to jagged operating conditions due to the discrete nature of the values of flux driving force used in the optimization problem. The WSO approach on the other hand simply sticks to the stationary operating point irrespective of external variations.

4.6.2 Case II: Intermittent solar profile

The intermittent solar profile allows us to observe the system's responses to alternating conditions. The values of solar radiation change from high to

low and back as shown in Figure 4.4(a). Such alternating solar profiles test the system's ability to switch between production and sustenance mode as and when it is necessary.

The plants responses are similar to those seen in the typical profile when the solar radiation initially increases from dawn. The output produced increases as the available power increases. It can be seen from Figure 4.4(b) that it produces output when the available power is above the threshold and ceases production during periods of low solar radiation by operating in sustenance mode. Understandably, the system consumes lesser power in sustenance mode as shown in 4.4(c). Although the variation of MDBR temperature is closely linked to power consumed and output produced as seen in Figure 4.4(d), one should note that there is a new development in terms of power consumed by the heat pump. Figure 4.4(e) shows a marked increase in the amount of power consumed by the heat pump around noon. This is due to the fact that the solar radiation is not sufficient to ensure survival of the micro-organisms in the MDBR tank. Thus, the system has been forced to rely on an external source of electricity to maintain the critical conditions required. Figures 4.4(f) and 4.4(g) show that the values of flow rate selected by the optimization problem also follow the pattern observed in the typical profile: minimum value for the feed loop and maximum value for the re-circulation loop.

General characteristics of PCO, RO and WSO remain the same. Variation of output produced and power consumed in PCO is smoother than those found in RO. WSO continues to remain at the same operating point irrespective of changes in solar profile.

4.6.3 Case III: Dark solar profile

The dark solar profile as the name suggests involves much lesser solar radiation than the other two profiles as shown by Figure 4.5(a). Hence, the available power values are also considerably lesser than the previous cases. During the brief period of solar radiation in the morning, the system switches to production mode to produce clean water as seen in 4.5(b). The solar radiation is not sufficient to support production during the rest of the day. Hence, the system operates in sustenance mode and power consumed is much lesser during the dark periods as seen in Figure 4.5(c). The general trend in performance continues in this profile also, even during the brief period of sunshine, PCO manages to produce more flux driving force than its counterparts. The system operates predominantly in sustenance mode as shown by Figure 4.5. As seen before, the power supplied to the heat pump increases when the solar radiation is not sufficient to maintain conditions required by the micro-organisms. There are no distinctions between PCO, RO and WSO in sustenance mode since, no optimization is involved. The system is operating under the influence of the regulatory layer alone.

4.6.4 Performance comparison

Figure 4.6 illustrates how effective each approach is at producing output and utilizing the power available. The ratio between the cumulative values of flux driving force and power available ($\Sigma J/\Sigma(Q_{load} + P_{load})$) can be used as a pragmatic indicator of performance. It is a measure of how well each approach makes use of the available resources to produce the maxi-

mum possible output. In other words, it indicates the flux driving force produced by consuming a single unit of power. To better understand the values obtained for this performance indicator we need to analyze the values of the intermediate quantities: cumulative flux driving force (ΣJ)and the cumulative power consumed ($\Sigma(Q_{load} + P_{load})$).

The first row of bar graphs show the values of cumulative flux driving force for each approach. Flux driving force for the typical profile is greater than the intermittent profile for all of the approaches. This can be explained through the difference in solar radiation available. The plant produces more output when more solar radiation is available. The same reasoning can be applied to the comparison of flux driving force produced by the intermittent and dark profiles. PCO produces more output than RO and WSO in all of the solar profiles considered.

The second row presents the cumulative value of power consumed in each situation. The dotted line bars represent the cumulative power available and the colored bars represent the cumulative power consumed. The PCO approach is able to adapt to changes in solar radiation and increase power consumed when power available increases. In theory, the PCO approach should have consumed all of the power available, but this is not the case in practice as shown by Figure 4.6. The difference between the actual power consumed and the power available is a consequence of the difference between the actual plant dynamics and the relaxations used during the formulation of the optimization problem. But, the results show that significant improvements in performance can be obtained in spite of these differences.

The third row presents the overall performance indicator for the approaches: the ratio between driving force and power consumed. It can be seen from Figure 4.6 that the ratio produced by PCO is higher than RO and WSO. This is an indication that if the value of power consumed is not accompanied by a proportional increase in flux driving force, then the system is not making the best use of the power available. Hence, PCO outperforms the other two approaches when subjected all of the three types of solar radiation profiles used in this study.

In addition to analyzing the results in terms of the performance indicators, one can also analyze the results in terms of the approaches studied, namely WSO, RO, and PCO. It is worth noting that they differ from each other by virtue of how the optimization problem is framed and also by virtue of how these approaches are put into practice. Analysis of the latter helps shed light on the results obtained.

Sections 4.4.2 explains that WSO determines a single stationary operating point. Section 4.4.3 states that, in the RO approach, "the optimization problem will minimize power consumed while forcing the output flux to take different values", this is meant to explain that multiple optimization problems will be solved with different values of flux as a constraint. Hence this will result in multiple operating points which form a set of possible options on how to operate the plant. During operation, the combination which is closest to the current reserve level is chosen as the control law. Section 4.4.4 explains that, the PCO approach, "involves solving a different optimization problem each time the operating points have to be determined". A different optimization problem will be solved each time since the bound

on the power consumption is linked to the time varying available reserve. The result of the optimization problem will correspond to a single optimal operating point for the current period. Since the optimization problem being solved each time is not the same, the operating points or solutions of the optimization problem are not predefined. These distinctions lay the basis for explaining that the results obtained need to be interpreted in terms of how they are applied in practice in addition to how the optimization problem is framed. We can now move on to the queries about the results obtained.

WSO performs worst in case of ΣJ since the stationary optimization problem chosen in Section 4.5.4 corresponds to a low value of flux driving force J. The explanation for this choice has been provided in the same section. It performs best in terms of $\Sigma(Q_{load} + P_{load})$ since the plant requires lesser power to produce lesser flux driving force. But, the power consumption is not small enough to raise the ratio between flux and power consumed, $\Sigma J/\Sigma(Q_{load} + P_{load})$, hence, WSO performs worst in this case also. The results from RO on the other hand are dependent on the number of optimization problems solved. In other words, dependent on the number of distinct values of output flux considered. RO performs better than WSO since it has the ability to determine operating points that correspond to a higher value of output flux than WSO. But the extent to which the power consumed is close to the available power is limited by the number of distinct values of flux. Hence RO does not perform better than PCO. In contrast, PCO incorporates the value of the available power into the optimization problem itself and hence is able to perform better than the other

two approaches.

4.7 Conclusion

The results indicate that the Power Constrained Optimization (PCO) approach outperforms the Repeated Optimization (RO) and Weighted Sum Optimization (WSO) approaches. PCO has demonstrated several areas of superiority. It produces more output, is able to make better use of the available power and is able to handle variations in solar radiation better. Hence, this approach is chosen as the most suitable to be incorporated in the control framework.

Analysis of the simulation results sheds light upon other aspects of the system also. These results are a better indicator of their ability to describe the plant than statistical tests. The simulation results show that even though the convex relaxations used in the optimization framework are not perfect, they allow the system to reap significant benefits in terms of performance. The simulations also illustrate that for truly self-sustaining operation the supervisory layer alone would not suffice. The system required assistance from an external source of electrical power whenever it encountered low solar radiation. The plant-wide control system must be able to accommodate such situations. Hence, these indications underscore the need for a scheduling layer to alleviate concerns about dependence on an external source of power.

4.8 Chapter summary

This chapter begins by presenting the objective behind the usage of the supervisory layer. The supervisory layer has to find the best balance between production rate and power consumed when the solar radiation is available in plenty. It also has to ensure survival of micro-organisms in the MDBR when solar radiation is not sufficient. For this purpose, it makes use of two modes: production and sustenance, which correspond to adequate and inadequate radiation respectively. Optimization of the control strategy can be done through various approaches as shown in Section 4.4. The different approaches considered are: weighted sum optimization, repeated optimization and power constrained optimization. In order to compare the effectiveness of each approach they have to be implemented and tested with simulations. Their implementation is not straight forward because of the presence of non convex terms in the optimization problem. Hence, methods to handle these incompatibilities and an analytical simulation framework to test the control strategies have been presented. The results obtained from each approach is then compared with the others for different solar radiation profiles. From the performance comparison it is evident that power constrained optimization outperforms the others. It is also evident that the plant-wide control system requires a back up reserve management system to be truly sustainable. Such a system will be discussed in the next chapter.

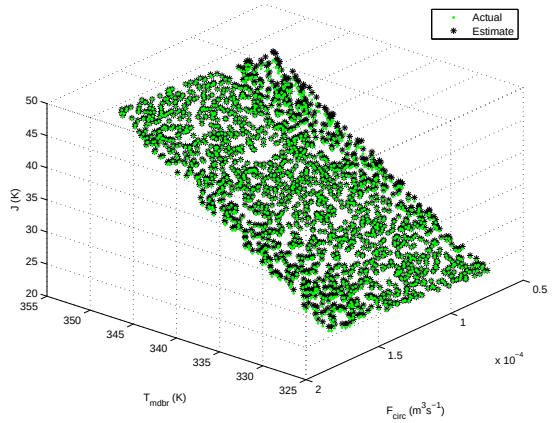

(a)

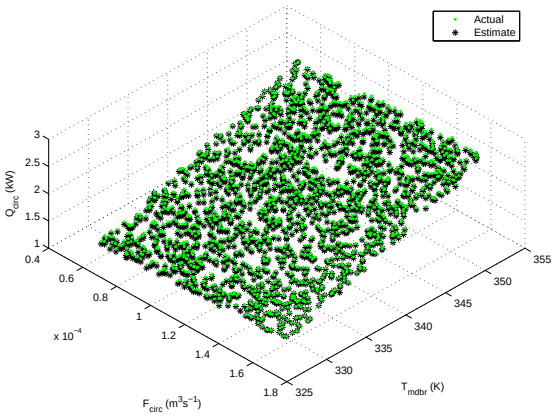

(b)

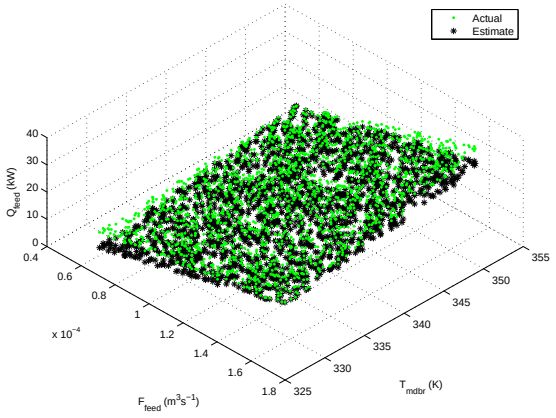

(c)

Figure 4.2: Three dimensional plots of the non convex terms (a) J (b) Q_{circ} (c) Q_{feed}

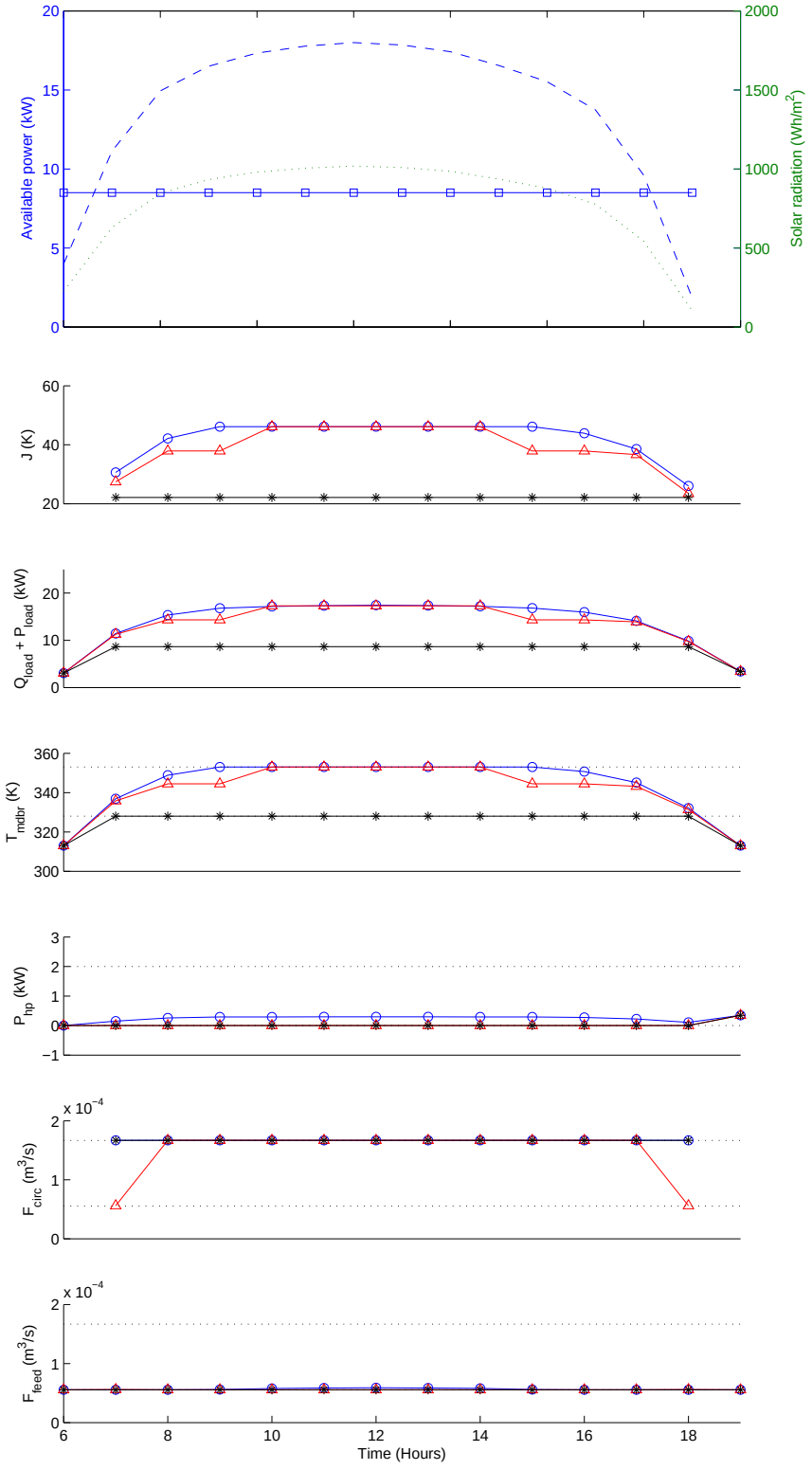

Figure 4.3: Supervisory layer - Typical solar profile

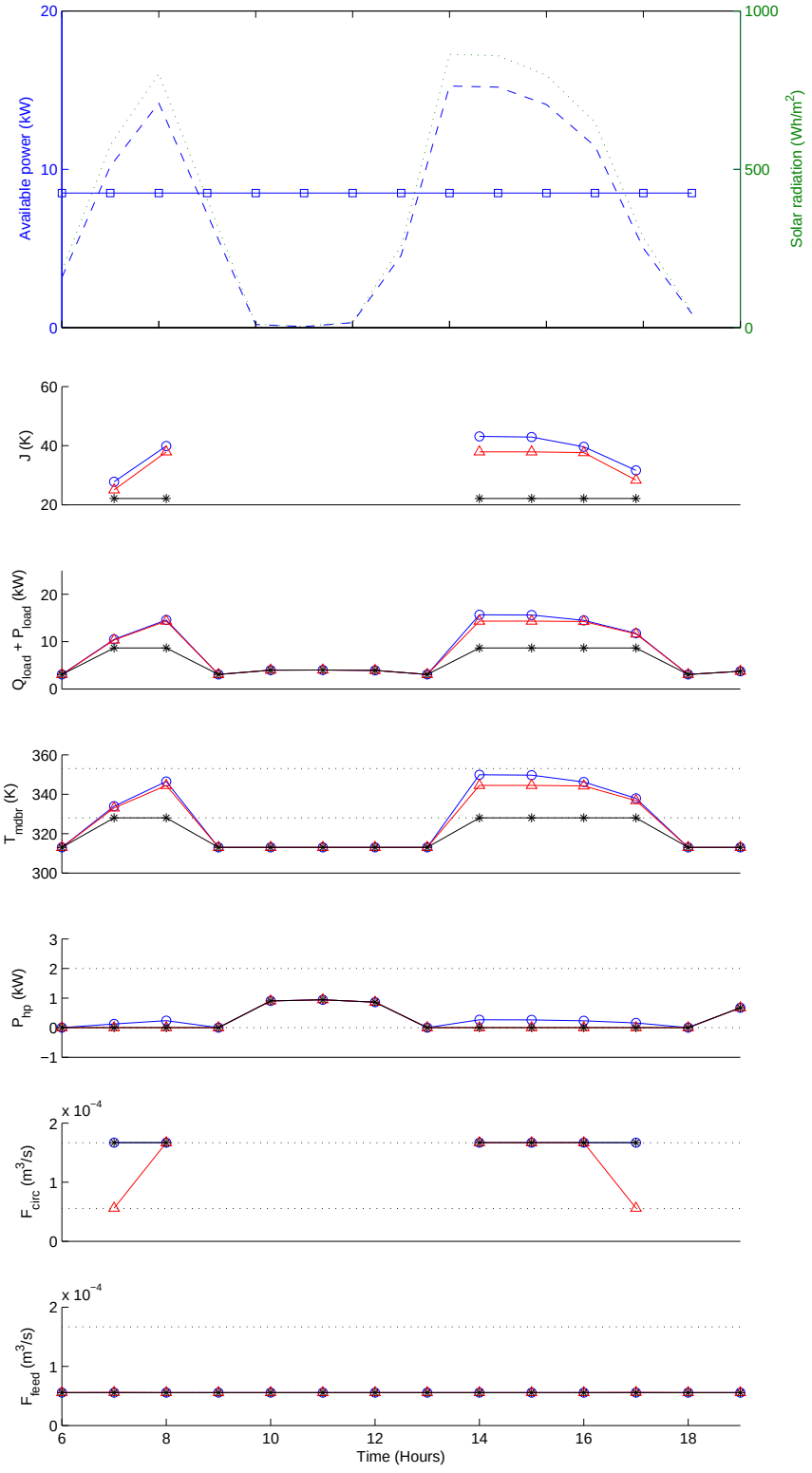

Figure 4.4: Supervisory layer - Intermittent solar profile

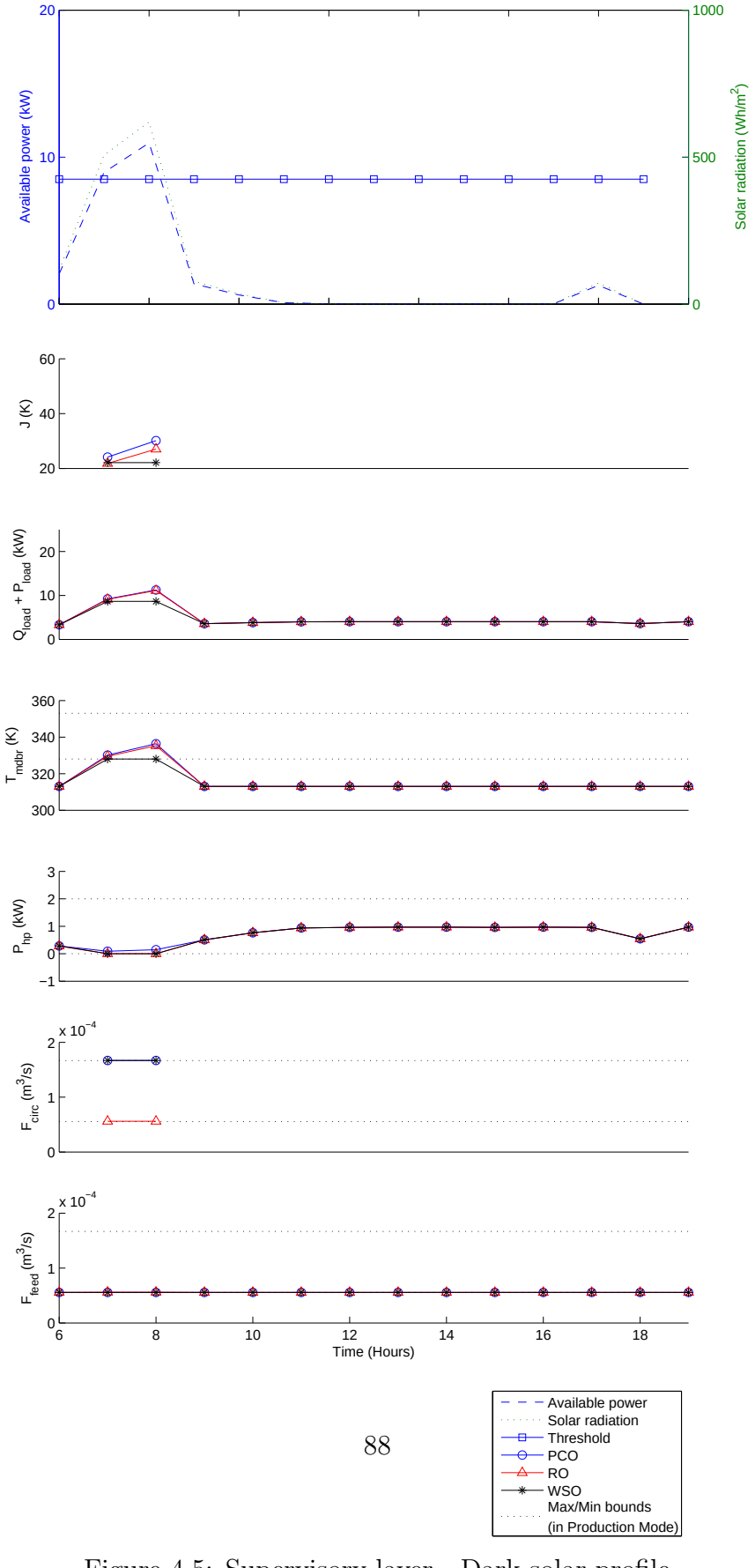

Figure 4.5: Supervisory layer - Dark solar profile

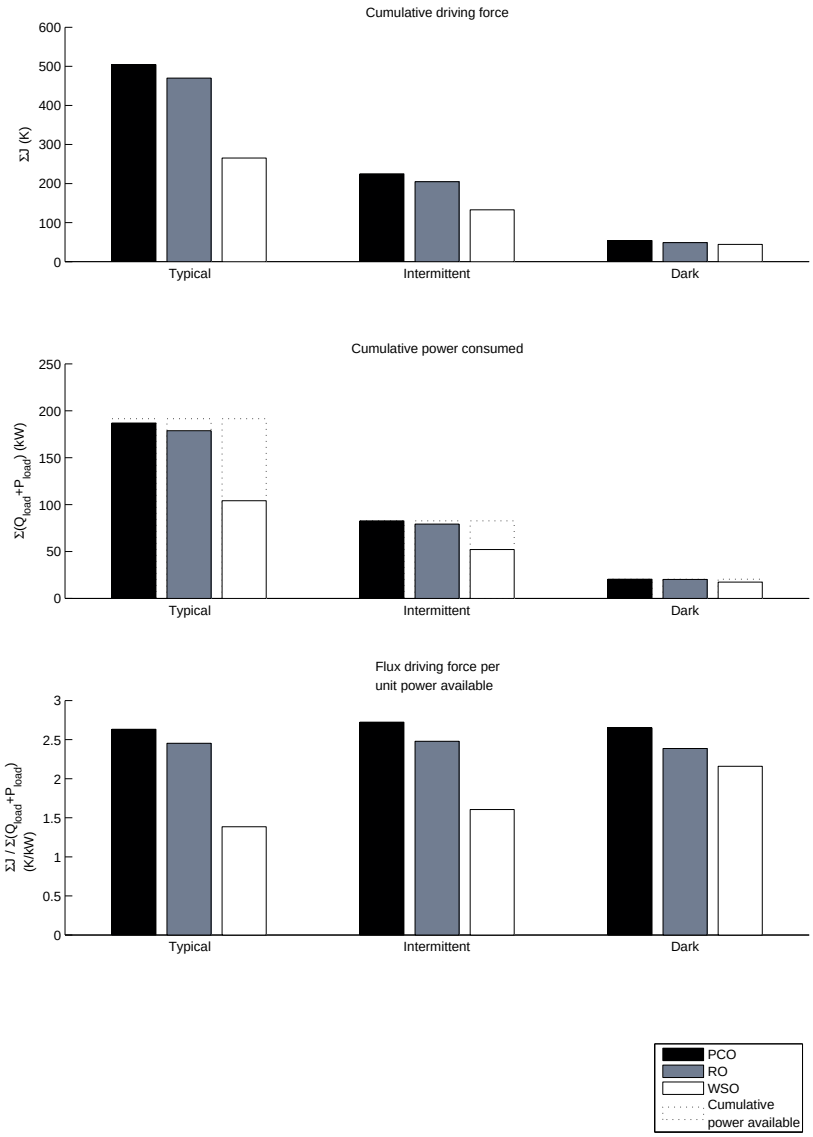

Figure 4.6: Supervisory Layer Comparison Chart

Chapter 5

Design and Evaluation of the Scheduling Layer

Energy reserves are managed by the scheduling layer. It ensures that the plant can maintain the conditions required for survival of MDBR bacteria even when it is subjected to unfavorable weather conditions. The scheduling layer will decide whether the plant can be allowed to consume all the power that is available or whether some of it has to be conserved for dark periods without sunlight. For this purpose, it needs to be aware of weather variations and requires information regarding the variation of solar radiation in the future. The scheduling layer will depend on the solar radiation prediction system to provide forecasts about the future.

The scheduling layer divides the interval between sunrise and sunset into three equal periods. It determines energy consumption targets for these periods based on information available from the solar radiation prediction system. These targets are revised when the prediction horizon is shifted

forward. For example, if the scheduling layer receives information about days one to five, it will use that information to compute consumption targets and a plan for the entire period from day one to day five. But, it will execute only the first target. In the next period, the scheduling layer will reassess the situation. It will use information about the current state of the system and the new set of forecasts to form another plan for days two to six. Again, it will execute only the first target and observe how the events unfold before computing the next set of targets. This process allows it to account for uncertainty in the forecasts and revise its strategy accordingly.

5.1 Feasibility condition

Before proceeding to solve the optimization problem, the system must check if the predicted data indicates that the problem is feasible. If the information from the prediction system indicates that the solar radiation will not be able to sustain even the minimum back up reserves required, the scheduling layer will not attempt to solve the optimization problem. This implies that if the predicted forecast does not allow the system to function continuously even if consumption targets for all intervals are set to the minimum value, then the scheduling layer will not attempt to solve the optimization problem. This is an indication that the problem is infeasible. But in case only some intervals have bad weather, then the scheduling layer is designed to help maximize the output produced. Hence it will only maintain the minimum back up reserves required for continuous operation i.e. save only what is necessary to ensure survival of microorganisms inside the MDBR.

5.2 Optimization problem

As in the supervisory layer, the scheduling layer optimization problem will also attempt to minimize a certain objective function $c(X, U)$ while satisfying a set of constraints $h(X, U) \leq 0$. The symbols x and u represent the state variables and the manipulated variables respectively. The general optimization takes the form:

$$\begin{aligned} \underset{U}{\text{minimize}} \quad & c(X, U) \\ \text{subject to} \quad & h(X, U) \leq 0 \end{aligned}$$

where the state variables $x_i \in X$ represent the predicted energy levels $w_i \in W$ and the manipulated variables $u_i \in U$ represent the energy consumption target for the i^{th} time period respectively. Hence,

$$X, U \in R^{N \times 1}$$

where N is the number of periods considered in the current planning horizon.

The decision variables or manipulated variables, $u_i \in U$ represent the energy consumption target for the i^{th} time period. These are different from the manipulated variables used in Chapter 4. The decision variables from the optimization problem in the Scheduling Layer will be used to enforce an upper bound on the energy consumption of the plant at different points of time. Thus these values are used to connect the supervisory and the scheduling layers. A more detailed discussion can be found in Section 5.4.

The special structure of the optimization problem discussed in this chapter can be exploited to reduce the complexity and computational effort required to determine the solution as shown in Appendix A.

5.2.1 Objective function

The system is designed to maximize output flux. It can be discerned from Section 4.6.4 that higher values of output flux require more energy consumption. If the system were to minimize the available reserves (r), it would be maximizing energy consumption. Expressions for the available reserve levels at the end of the i^{th} period are described as follows:

$$r_i = r_{i-1} + w_i - u_i \tag{5.1}$$

where w_i represents the predicted energy level and u_i represents the consumption target for the i^{th} period as mentioned earlier. Equation 5.1 defines the available reserves, r_i, as the difference between the energy available and the energy consumed. Hence, the objective function takes the form:

$$\underset{U}{\text{minimize}} \left[\sum_{i=1}^{N} (r_i) \right] \tag{5.2}$$

5.2.2 Constraints

The constraints are formulated as follows:

$$r_i \geq e_s \qquad i = 1, \ldots, N \tag{5.3}$$

$$e_p \geq u_i \geq e_s \qquad i = 1, \ldots, N \tag{5.4}$$

Equation 5.3 makes sure that the available reserve should always be greater than the load required to support plant operation in sustenance mode, e_s. Equation 5.4 ensures that the scheduling targets lie between their upper and lower bounds. The upper bound is the maximum consumption possible in production mode , e_p. The lower bound should obviously be the consumption level required to sustain plant operation in sustenance mode, e_s. Since all functions and constraints are compatible with the disciplined convex programming rule set they do not require any modifications.

Remark

The optimization problem discussed above considers values of consumption targets in between the maximum value possible in production mode e_p and the minimum value required to sustain bacteria e_s. In principle, the results obtained by solving this optimization problem can result in targets that are in between the threshold required to operate in production mode and the minimum required for sustenance of micro-organisms. In such situations, the supervisory layer will merely operate in sustenance mode and the plant will transfer the unused energy to the reserve.

5.3 Results and discussion

The procedure in the closed loop simulation block diagram from Figure 5.1 has been implemented in Matlab. The parameters specified in Table 5.1 were used. This was done while using actual solar radiation data for three different weeks from the sources mentioned in Section 4.6 using Matlab. The

values of e_s, e_p and time interval between change in manipulated variables is given in Table 5.1.As in the case of the supervisory layer, these generic solar profiles have been selected such that they are representative of the different scenarios the scheduling layer is likely to encounter. These profiles also consist of typical, intermittent and dark variants. In this case, the time frame considered is larger (in terms of weeks). The typical, intermittent and dark profiles are characterized by consistent, irregular and low levels of solar radiation respectively.

Table 5.1: Scheduling layer parameters

Quantity	Value
Sustenance bound (e_s)	34 kWh
Production bound (e_p)	88 kWh
No. of solar predictions (N)	15
No. of days in planning horizon	5
Time interval between change in control strategy (sampling period)	4 hours (= (5/15) * (12 hours of sunshine))

5.3.1 Case I: Typical profile

In the case of the typical profile, the scheduling layer realizes that a steady source of solar radiation is available on days other than the first day as seen in the first row of Figure 5.2. Hence, it gives itself the liberty of consuming more energy on days with more solar radiation as seen in the second row of Figure 5.2. As a consequence of these consumption targets, the reserve levels tend to be relatively higher during the first day and remain at the the minimum level of system reserve required through the rest of the week.

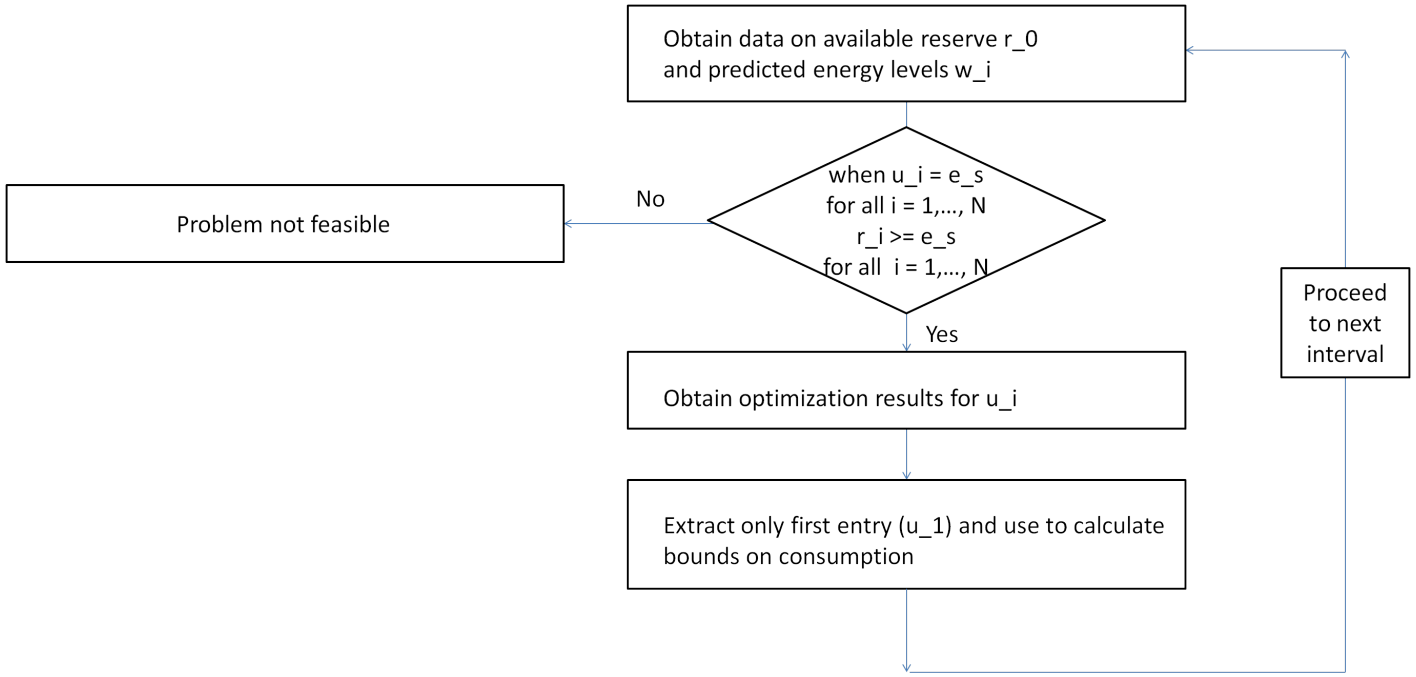

Figure 5.1: Simulation block diagram - Scheduling layer

This allows the plant to support the load required to ensure survival of bacteria.

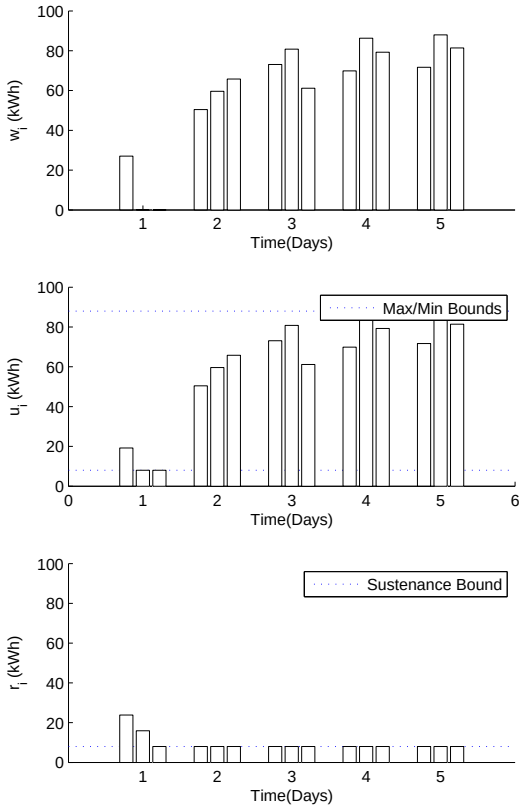

Figure 5.2: Scheduling Layer - Typical profile

5.3.2 Case II: Intermittent profile

The intermittent profile characterized by bursts of radiation between dark periods as shown in the first row of Figure 5.3. As the predictions indicate lower solar radiation levels, the consumption targets decrease as shown in the second row of Figure 5.3. The scheduling layer increases these targets only marginally during periods of adequate radiation in order to conserve for the future. The reserve levels are increased in preparation for low radiation

as seen in the third row. Thus the scheduling layer is able to make sure that undesirable periods can be handled with sufficient reserves.

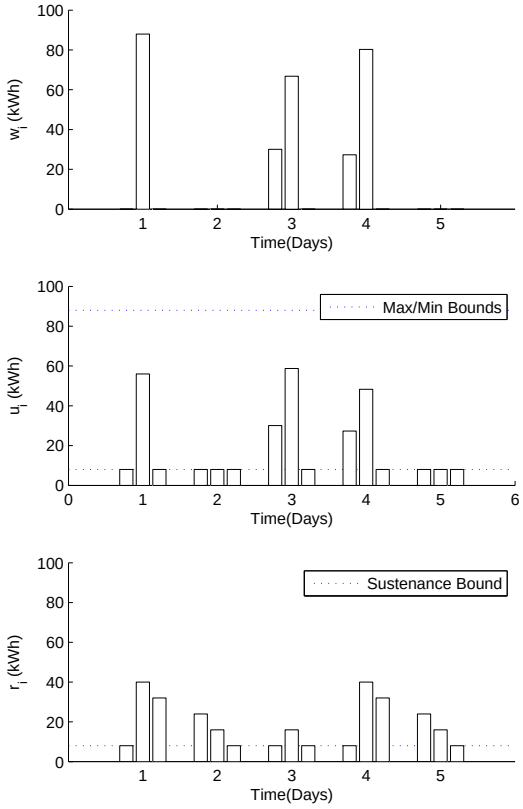

Figure 5.3: Scheduling Layer - Intermittent profile

5.3.3 Case III: Dark profile

The dark profile offers very little scope for production of clean water. The forecasts indicate mostly unfavorable conditions and low solar radiation as shown in the first row of Figure 5.4. The scheduling layer adopts a conservative strategy when it knows that the weeks ahead will not encounter sunshine. The consumption targets determined are much lower than those observed in the previous profiles as shown in the second row of Figure 5.4.

Only through adoption of such a strategy is it able to make sure that the plant has enough reserves to operate in sustenance mode without external assistance.

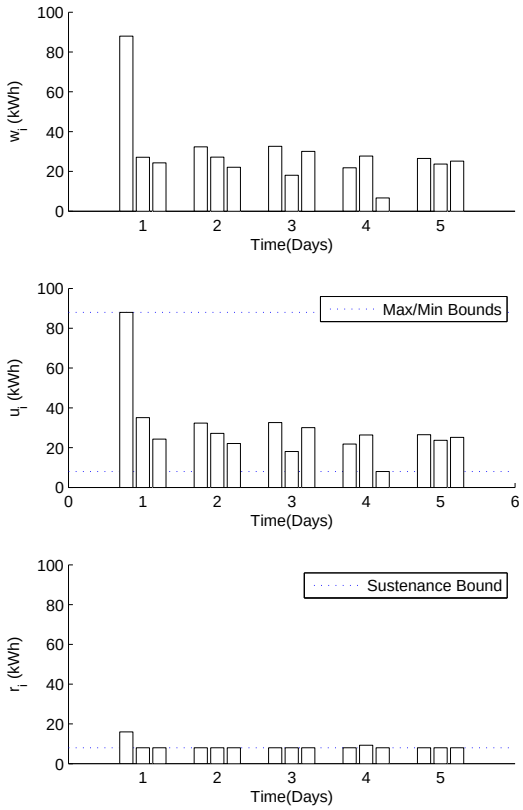

Figure 5.4: Scheduling Layer - Dark profile

5.4 Conclusion

The main conclusion that can be arrived from the results shown in the previous section is that the scheduling layer is capable of determining an effective consumptions strategy that will allow the plant to function continuously even when subjected to a variety of solar predictions or profiles.

The scheduling layer's design and structure also allows us to decide how it will integrate with the supervisory layer. The scheduling layer will enforce an upper bound on the amount of energy that can be consumed during different points of time. These bounds can be readily incorporated in to the constraints of the online optimization problem described in Section 4.4.4 by making use of the following relations:

$$\begin{aligned} Q_{bound} &= min(Q_{available}, Q_{sch}) \\ P_{bound} &= min(P_{available}, P_{sch}) \end{aligned}$$

where the subscript *sch* refers to the target set by the scheduling layer. Thus, in case the current solar radiation levels are high but the forecasts indicate bad weather, the plant will conserve energy. If the actual level of solar radiation is lower than the scheduling target , the system will proceed to consume all the energy that is available.

When used in conjunction with RO, there is a possibility that the operating points selected by the supervisory layer may not match those determined by the scheduling layer. Hence, this can lead to a mismatch between the layers. If the scheduling layer were to take this discrete nature of the RO formulation into account in its optimization problem, it would have to make use of a Mixed Integer Program(MIP). MIPs are non-convex and hence cannot guarantee that the solution determined is the optimal solution for the given problem unless an exhaustive search is executed. In the light of these shortcomings and superior performance, PCO and the scheduling layer are deemed to be the best choices for the plant-wide control system.

5.5 Chapter summary

This chapter begins with the feasibility condition that ensures that the problem can be solved. In case the forecast points that minimum reserves cannot be maintained even if minimum consumption targets are set, then the scheduling layer will not attempt to solve the optimization problem. Upon satisfying this condition, the scheduling layer moves on the optimization problem, which involves minimizing the overall reserve while keeping the individual reserve within the specified lower and upper bounds. This optimization problem is used with solar prediction data to demonstrate the results obtained. The chapter concludes by explaining the scheduling layer's significance and how it integrates into the supervisory layer.

Chapter 6

Conclusion

6.1 Summary

This thesis provides an introduction to the formulation and design of a plant-wide control system for the solar powered MDBR plant. The objectives that motivated control were safety, self sustaining operation and maximization of output produced. The system must determine a control strategy that best utilizes the energy available from the sun to produce clean water. It must also bear in mind that while doing so, the plant also has to accumulate enough reserves to ensure the survival of the essential micro-organisms in the MDBR during periods of inadequate solar radiation. The main focus of this thesis is the formulation of convex optimization problems that can help determine the control strategies which will satisfy these objectives. This is done by first going through the background information necessary on water reclamation, convex optimization and plant-wide control in general. Then the thesis moves on to a discussion of the solar pow-

ered MDBR plant and hierarchical control framework under consideration. The design and evaluation of the layers of the hierarchical framework which require optimization, namely, the scheduling and supervisory layers are covered in the subsequent chapters. The scheduling layer problem makes sure that the control strategy plans its back up reserve allocation several days ahead of unfavorable weather. This optimization problem has been shown to be suitable for convex algorithms in its original form. Hence it can be readily solved through the use of convex optimization. The supervisory layer problem governs real time optimization and mode selection. Different approaches have been considered and compared for this layer, namely, Power Constrained Optimization (PCO), Repeated Optimization (RO) and Weighted Sum Optimization (WSO). PCO solves a different optimization problem at each period, RO solves multiple optimization problems to form a set of possible operating points and WSO optimizes a weighted sum of output flux and the power consumed. Out the approaches considered, PCO has been deemed to be superior since it outperforms the other two approaches and can be easily integrated with the scheduling layer. In addition to this, the thesis also covers the modifications required to incorporate the non convex terms present in the supervisory layer into convex optimization problems. Simulation studies are performed to demonstrate the performance of the proposed control framework through illustrative examples. The results obtained from the illustrative examples show that the control system is capable of improving and extending the automated functions of the plant. Implementation of the proposed control system will greatly reduce the need for operator intervention and maintenance activities. The layered structure

can accommodate future modifications and inclusion of better functions can be established without having to incur the costs of overall replacement.

6.2 Future work

The performance of the system can be improved further by dealing with some issues related to the supervisory and scheduling layers:

The MDBR is not designed to handle rapid changes in operating conditions. The practical constraints that can limit the usefulness of the proposed approach are tied to the MDBR. In order to leverage on the computation that can be performed in real-time, the control strategies have to be adjusted according to variations in solar radiation. But in the current setup, changes in solar radiation are faster than the changes in operating conditions. This is because current industry practice suggests that trends are rather slow in the MDBR due to system capacitance[32]. Hence, to take full advantage of the computations that can be performed by the proposed framework, further research is required to assess the minimum time interval between changes in operating conditions for MDBRs.

The model can be extended to account for transients in membrane performance due to fouling. The fouling is caused by gradual deposition of particles and macro-solutes on the membrane surface [54]. This effect will be incorporated into the required driving force as a function of time. Fouling can usually be reversed by regular cleaning.

Al though the Power Constrained Optimization (PCO) approach reduces the computation load, it still requires an online optimization solver.

If such software complexity is not desirable, a look-up table can be used to decrease online computation. The look-up table has to be generated by solving a series of optimization problems similar to the one discussed in Section 4.4.4. Each of these problems will correspond to different values of bounds on the power consumed as follows:

$$\begin{aligned} \underset{U}{\text{maximize}} \quad & J \\ \text{subject to} \quad & Q_{load} \leq Q_i \in [Q_{min}, Q_{max}] \\ & P_{load} \leq P_j \in [P_{min}, P_{max}] \\ & \underline{U} \leq U \leq \overline{U} \end{aligned}$$

The solutions thus obtained will be stored as separate entries in the look-up table. In practice, the system may encounter values of Q_i and P_j which were not used while generating the look-up table. In such situations interpolation will be used to determine the operating point. Thus this approach significantly decreases the amount of online computation required by restricting itself to interpolation.

Hence, further studies are necessary to resolve the above mentioned issues.

Bibliography

[1] J. Phattaranawik, A. Fane, A. Pasquier, and W. Bing, "A novel membrane bioreactor based on membrane distillation," *Desalination*, vol. 223, no. 1-3, pp. 386–395, 2008.

[2] A. Criscuoli, M. Carnevale, and E. Drioli, "Evaluation of energy requirements in membrane distillation," *Chemical Engineering and Processing: Process Intensification*, vol. 47, no. 7, pp. 1098–1105, 2008.

[3] S. Lee and H. Kim, "Optimal operating policy of the ultrafiltration membrane bioreactor for enzymatic hydrolysis of cellulose," *Biotechnology and bioengineering*, vol. 42, no. 6, pp. 737–746, 1993.

[4] J. Liu and Z. Cui, "Optimization of operating conditions for glucose oxidation in an enzymatic membrane bioreactor," *Journal of Membrane Science*, vol. 302, no. 1-2, pp. 180–187, 2007.

[5] T. Mohammadi and M. Safavi, "Application of taguchi method in optimization of desalination by vacuum membrane distillation," *Desalination*, vol. 249, no. 1, pp. 83–89, 2009.

[6] V. A. Bui, L. T. T. Vu, and M. H. Nguyen, "Simulation and optimisation of direct contact membrane distillation for energy efficiency," *Desalination*, vol. 259, no. 1-3, pp. 29–37, 2010.

[7] L. Cheng, P. Wu, and J. Chen, "Modeling and optimization of hollow fiber dcmd module for desalination," *Journal of Membrane Science*, vol. 318, no. 1-2, pp. 154–166, 2008.

[8] M. Khayet, C. Cojocaru, and M. García-Payo, "Experimental design and optimization of asymmetric flat-sheet membranes prepared for direct contact membrane distillation," *Journal of Membrane Science*, vol. 351, no. 1-2, pp. 234–245, 2010.

[9] S. Yoon, H. Kim, and I. Yeom, "Optimization model of submerged hollow fiber membrane modules," *Journal of Membrane Science*, vol. 234, no. 1-2, pp. 147–156, 2004.

[10] H. Chang, G. B. Wang, Y. H. Chen, C. C. Li, and C. L. Chang, "Modeling and optimization of a solar driven membrane distillation desalination system," *Renewable Energy*, vol. 35, no. 12, pp. 2714–2722, 2010.

[11] A. Vijay, K. V. Ling, and A. G. Fane, "Applications of convex optimization in plant-wide control of membrane distillation bio-reactor (MDBR) water recycling plant," *Proceedings of the 11th International Conference on Control, Automation, Robotics and Vision (ICARCV 2010)*, pp. 246–251, 2010.

[12] J. G. March, M. Gual, and F. Orozco, "Experiences on greywater reuse for toilet flushing in a hotel (mallorca island, spain)," *Desalination*, vol. 164, no. 3, pp. 241–247, 2004.

[13] D. Christova-Boal, R. E. Eden, and S. McFarlane, "An investigation into greywater reuse for urban residential properties," *Desalination*, vol. 106, no. 1-3, pp. 391–397, 1996.

[14] B. Jefferson, A. Laine, S. Parsons, T. Stephenson, and S. Judd, "Technologies for domestic wastewater recycling," *Urban water*, vol. 1, no. 4, pp. 285–292, 2000.

[15] A. Amokrane, C. Comel, and J. Veron, "Landfill leachates pretreatment by coagulation-flocculation," *Water Research*, vol. 31, no. 11, pp. 2775–2782, 1997.

[16] A. Tatsi, A. Zouboulis, K. Matis, and P. Samaras, "Coagulation-flocculation pretreatment of sanitary landfill leachates," *Chemosphere*, vol. 53, no. 7, pp. 737–744, 2003.

[17] M. Drikas, C. Chow, J. House, and M. Burch, "Using coagulation, flocculation, and settling to remove toxic cyanobacteria," *Journal American Water Works Association*, vol. 93, no. 2, pp. 100–111, 2001.

[18] W. Glaze, J. Kang, and D. Chapin, "The chemistry of water treatment processes involving ozone, hydrogen peroxide and ultraviolet radiation," *Ozone: Science & Engineering*, vol. 9, no. 4, pp. 335–352, 1987.

[19] W. Glaze, F. Beltran, T. Tuhkanen, and J. Kang, "Chemical models of advanced oxidation processes," *Water Pollution Research Journal of Canada*, vol. 27, no. 1, pp. 23–42, 1992.

[20] M. Stefan, J. Mack, and J. Bolton, "Degradation pathways during the treatment of methyl tert-butyl ether by the UV/H2O2 process," *Environ. Sci. Technol*, vol. 34, no. 4, pp. 650–658, 2000.

[21] A. Pabby, S. Rizvi, and A. Sastre, *Handbook of membrane separations: chemical, pharmaceutical, food, and biotechnological applications.* CRC, 2008.

[22] S. Judd and C. Judd, *The MBR book: principles and applications of membrane bioreactors in water and wastewater treatment.* Elsevier Science Ltd, 2006.

[23] B. Bodell, "Silicone rubber vapour diffusion in saline water distillation," *United States Patent Serial No 1963*, vol. 285, 1963.

[24] M. Findley, "Vaporization through porous membranes," *Industrial Engineering Chemistry Process Design and Development*, vol. 6, no. 2, pp. 226–230, 1967.

[25] M. El-Bourawi, Z. Ding, R. Ma, and M. Khayet, "A framework for better understanding membrane distillation separation process," *Journal of Membrane Science*, vol. 285, no. 1-2, pp. 4–29, 2006.

[26] K. Lawson and D. Lloyd, "Membrane distillation," *Journal of Membrane Science*, vol. 124, no. 1, pp. 1–25, 1997.

[27] J. Bailey, "Shipboard sewage treatment system." DTIC Document, Tech. Rep., 1971.

[28] K. Yamamoto, M. Hiasa, T. Mahmood, and T. Matsuo, "Direct solid-liquid separation using hollow fiber membrane in an activated sludge aeration tank," *Water Science and Technology WSTED 4*, vol. 21, no. 4-5, 1989.

[29] P. Le-Clech, V. Chen, and A. G. Fane, "Fouling in membrane bioreactors used in wastewater treatment," *Journal of Membrane Science*, vol. 284, no. 1-2, pp. 17–53, 2006.

[30] T. Bae and T. Tak, "Interpretation of fouling characteristics of ultrafiltration membranes during the filtration of membrane bioreactor mixed liquor," *Journal of Membrane Science*, vol. 264, no. 1-2, pp. 151–160, 2005.

[31] J. Phattaranawik, A. Fane, A. Pasquier, W. Bing, and F. Wong, "Experimental study and design of a submerged membrane distillation bioreactor," *Chemical Engineering and Technology*, vol. 32, no. 1, pp. 38–44, 2009.

[32] T. H. Khaing, J. Li, Y. Li, N. Wai, and F. S. Wong, "Feasibility study on petrochemical wastewater treatment and reuse using a novel submerged membrane distillation bioreactor," *Separation and purification Technology*, vol. 74, no. 1, pp. 138–143, 2010.

[33] J. Choi, S. Dockko, K. Fukushi, and K. Yamamoto, "A novel application of a submerged nanofiltration membrane bioreactor (NF MBR)

for wastewater treatment," *Desalination*, vol. 146, no. 1-3, pp. 413–420, 2002.

[34] A. Goetzberger and V. Hoffmann, *Photovoltaic solar energy generation*. Springer Verlag, 2005, vol. 112.

[35] B. Lindgren, "Power-generation, power-electronics and power-systems issues of power converters for photovoltaic applications," Ph.D. dissertation, Chalmers University of Technology, 2002.

[36] A. Fiacco and G. McCormick, *Nonlinear programming*. Wiley New York, 1968.

[37] I. Dikin, "Iterative solution of problems of linear and quadratic programming," *Soviet Mathematics Doklady*, vol. 8, no. 3, pp. 674–675, 1967.

[38] N. Karmarkar, "A new polynomial-time algorithm for linear programming," *Combinatorica*, vol. 4, no. 1984, pp. 373–395, 1984.

[39] Y. Nesterov and A. Nemirovskii, *Interior-point polynomial algorithms in convex programming*. Society for Industrial Mathematics, 1987.

[40] S. Boyd and L. Vandenberghe, *Convex optimization*. Cambridge Univ Pr, 2004.

[41] T. Larsson and S. Skogestad, "Plantwide control-a review and a new design procedure," *Modeling Identification and Control*, vol. 21, no. 4, pp. 209–240, 2000.

[42] G. Stephanopoulos and C. Ng, "Perspectives on the synthesis of plant-wide control structures," *Journal of Process Control*, vol. 10, no. 2-3, pp. 97–111, 2000.

[43] M. Morari, Y. Arkun, and G. Stephanopoulos, "Studies in the synthesis of control structures for chemical processes: Part I: Formulation of the problem. process decomposition and the classification of the control tasks. analysis of the optimizing control structures," *AIChE Journal*, vol. 26, no. 2, pp. 220–232, 1980.

[44] S. Skogestad, "Control structure design for complete chemical plants," *Computers and Chemical Engineering*, vol. 28, no. 1-2, pp. 219–234, 2004.

[45] J. Morud and S. Skogestad, "Effects of recycle on dynamics and control of chemical processing plants," *Computers & chemical engineering*, vol. 18, pp. S529–S534, 1994.

[46] E. Gilliland, L. Gould, and T. Boyle, "Dynamic effects of material recycle," *Prepr. JACC, Stanford, CA*, pp. 140–146, 1964.

[47] H. Carlemalm, "Studies on controllability of integrated process systems," Ph.D. dissertation, KTH, Signals, Sensors and Systems, 2003.

[48] L. Martinez and F. Florido-Diaz, "Theoretical and experimental studies on desalination using membrane distillation," *Desalination*, vol. 139, no. 1-3, pp. 373–379, 2001.

[49] R. Palgrave, *Troubleshooting centrifugal pumps and their systems*. Elsevier Science Ltd, 2003.

[50] M. Abdelghani-Idrissi, M. Arbaoui, L. Estel, and J. Richalet, "Predictive functional control of a counter current heat exchanger using convexity property," *Chemical Engineering and Processing*, vol. 40, no. 5, pp. 449–457, 2001.

[51] A. Thumann and D. Mehta, *Handbook of energy engineering*. The Fairmont Press, Inc., 2001.

[52] B. Ogunnaike and W. Ray, *Process Dynamics, Modeling, and Control*. Oxford University Press, USA, 1994.

[53] M. Grant, S. Boyd, and Y. Ye, "CVX: Matlab software for disciplined convex programming," *avialable at http://www. stanford. edu/boyd/cvx*, vol. 1.

[54] J. Zhang, H. Chua, J. Zhou, and A. Fane, "Factors affecting the membrane performance in submerged membrane bioreactors," *Journal of Membrane Science*, vol. 284, no. 1-2, pp. 54–66, 2006.

Appendix A

Reduced Complexity Algorithm for the Scheduling Layer

A.1 Analysis and discussion of problem structure

Further analysis of the scheduling layer optimization problem reveals that, it can be solved without the use of an online optimization solver. The structure of the problem allows us to define an algorithm of reduced complexity to determine the optimal solution. Expansion of all of the expressions in equations 5.1 to 5.4 is essential for understanding the nature of the optimization problem. By definition, the reserve levels from different periods according to equation 5.1 are:

$$
\begin{aligned}
r_1 &= r_0 + w_1 - u_1 \\
r_2 &= r_1 + w_2 - u_2 \\
&= r_0 + w_1 - u_1 + w_2 - u_2 \\
&= r_0 + \sum_{i=1}^{2}(w_i - u_i) \\
r_3 &= r_2 + w_3 - u_3 \\
&= r_0 + w_1 - u_1 + w_2 - u_2 + w_3 - u_3 \\
&= r_0 + \sum_{i=1}^{3}(w_i - u_i)
\end{aligned}
$$

Hence,

$$r_n = r_0 + \sum_{i=1}^{n}(w_i - u_i) \tag{A.1}$$

From the above equation one can deduce that the objective function from 5.2,

$$\underset{U}{\text{minimize}} \left[\sum_{i=1}^{N}(r_i)\right]$$

can be expressed as,

$$\underset{U}{\text{minimize}} \left[\sum_{i=1}^{N}\left(r_0 + \sum_{j=1}^{i}(w_j - u_j)\right)\right]$$

or,

$$\underset{U}{\text{minimize}} \left[Nr_0 + \sum_{i=1}^{N}\left((N+1-i)(w_i - u_i)\right)\right]$$

or,

$$\underset{U}{\text{minimize}} - c^T U + d \tag{A.2}$$

where $c = \begin{bmatrix} N & N-1 & N-2 & \cdots & 1 \end{bmatrix}^T$ and $d = Nr_0 + \sum_{i=1}^{N}(N+1-i)w_i$. Thus the original objective function can be equivalently formulated as maximization of a linear function of the optimization variable. Equation A.1 also illustrates that the constraint from Equation 5.3 can be written as,

$$R_0 + LW - LU \geq E_s$$

where

$$\begin{aligned}
R_0 &= \begin{bmatrix} r_0 & r_0 & \cdots & r_0 \end{bmatrix}^T \\
W &= \begin{bmatrix} w_1 & w_2 & \cdots & w_N \end{bmatrix}^T \\
U &= \begin{bmatrix} u_1 & u_2 & \cdots & u_N \end{bmatrix}^T \\
E_s &= \begin{bmatrix} e_s & e_s & \cdots & e_s \end{bmatrix}^T \\
L &= \begin{bmatrix} 1 & 0 & 0 & \cdots & 0 \\ 1 & 1 & 0 & \cdots & 0 \\ 1 & 1 & 1 & \ddots & 0 \\ \vdots & & & \ddots & 0 \\ 1 & 1 & 1 & \cdots & 1 \end{bmatrix}
\end{aligned}$$

. By re-arranging the terms and multiplying both sides of the above equation by L^{-1} we get,

$$L^{-1}(R_0 - E_s) + W \geq U \tag{A.3}$$

Equation A.3 makes up a key element of the solution algorithm. All the elements on the left hand side of the equation are constants and represent the maximum values that components of the vector u can take. Hence by replacing the inequality by an equality sign and solving the set of simultaneous equations, one can obtain a preliminary estimate of the solution of the optimization problem without the use of an optimization solver. This solution is referred to as the preliminary estimate since it does not take into account the upper and lower bounds imposed upon the optimization variable by equation 5.4. In other words, this estimate can contain values that may either be higher than the plant's designed capacity or may be lower than the value required for operation in sustenance mode. Hence, some adjustment is required to ensure that the values of the optimization variables do not violate these constraints. This is done in two stages.

In the first stage of adjustment, the variables u_i are analyzed starting from u_1 to u_N. If at any variable, there is a surplus or excess above the maximum bound, this surplus is shifted to the subsequent interval. This process removes any violations of the constraint related to the upper bound. In the second stage of adjustment, the variables u_i are analyzed from u_N to u_2. If at any variable, there is a deficit or gap below the minimum bound, this deficit is borrowed from the interval preceding the current interval. Performing these steps for all variables up till u_2 will remove any violations of the lower bound. Notice that the second stage of adjustment is not allowed to modify u_1. This has been done to check whether the problem is feasible. If the second stage of adjustments results in a value of $u_1$that is lesser than the minimum bound, then it is obvious that the predicted values

are not sufficient to sustain the minimum reserve levels required during all periods. In such cases, the problem is deemed to be infeasible.

The rationale behind the operation of this algorithm can be understood through the structure of the original scheduling layer problem. The initial estimate has been determined through manipulation of the inequality present in the original problem. The only aspects that equation A.3 does not consider are the bounds on the optimization variable. Hence after computing this initial estimate, the problem reduces to re-distributing the excess or deficit such that the constraints are satisfied. The maximum bound signifies that the consumption cannot be above a certain value since that represents the physical limits of the plant. Hence, if radiation available is more than what the plant can use, any surplus will obviously be transferred to the reserve to be used the next day. This is the principle behind the first stage of surplus adjustment. As for the second stage, if the consumption is below the minimum required at any interval, it is an indication that additional reserves have to be saved up before that point of time. Hence, borrowing the deficit from the preceding intervals, the second adjustment accomplishes that goal. Thus the algorithm has been reduced to a series of simple mathematical operations as shown in the next section.

A.2 Algorithm sequence

The matlab code for the algorithm described in this Appendix is as follows:

```
u_alg = inv(L)*((r0-es)*ones(n,1))+W;
```

```
%if there is surplus in the current period,
%store it as reserve and use in the next period
for i=1:n
    if u_alg(i) > ep
        u_alg(i+1) = u_alg(i+1) + (u_alg(i) - ep);
        u_alg(i) = ep;
    end
end

%if there is deficit in the current period,
%use less in the previous period
for i=n:-1:2
    if u_alg(i) < es
        u_alg(i-1) = u_alg(i-1) - (es - u_alg(i));
        u_alg(i) = es;
    end
end

if u_alg(1) < es, disp('Problem Infeasible!'), end
```

In relative terms, first statement of the algorithm requires more computational effort since it involves matrix inversion, L^{-1}. Since L is constant it can easily be determined beforehand and incorporated into the algorithm. But in this case if the size of the problem changes (i.e. the number of predictions available changes), the inverse of the new matrix has to be de-

termined before this algorithm can be used. The next section proves that even the operations required for determining L^{-1} can be reduced through an explicit inversion procedure.

A.3 Explicit inversion proof

To prove

$$\left[A^{(n)}\right]^{-1} = B^{(n)} \tag{A.4}$$

where $A^{(n)}$ is a $n \times n$ lower triangular matrix of the form:

$$\begin{bmatrix} 1 & 0 & 0 & \cdots & 0 \\ 1 & 1 & 0 & \ddots & 0 \\ 1 & 1 & 1 & \ddots & \vdots \\ \vdots & & & \ddots & 0 \\ 1 & 1 & 1 & \cdots & 1 \end{bmatrix}_{n \times n}$$

and $B^{(n)}$ is a $n \times n$ matrix of the form:

$$\begin{bmatrix} 1 & 0 & 0 & \cdots & 0 \\ -1 & 1 & 0 & \ddots & 0 \\ 0 & -1 & 1 & \ddots & \vdots \\ \vdots & \ddots & \ddots & \ddots & 0 \\ 0 & \cdots & 0 & -1 & 1 \end{bmatrix}_{n \times n}$$

Proof

When n=1,

$$A^{(n)} = A^{(1)} = [1]$$

we know,

$$\left[A^{(1)}\right]^{-1} = [1] = B^{(1)}$$

hence equation A.4 is valid for n=1. When n=2

$$A^{(n)} = A^{(2)} = \begin{bmatrix} 1 & 0 \\ 1 & 1 \end{bmatrix}$$

we know,

$$\left[A^{(2)}\right]^{-1} = \begin{bmatrix} 1 & 0 \\ -1 & 1 \end{bmatrix} = B^{(2)}$$

hence equation A.4 is valid for n=2. Let equation A.4 be valid for some value n=k, which implies that

$$\left[A^{(k)}\right]^{-1} = B^{(k)} \tag{A.5}$$

For n=k+1,

$$A^{(k+1)} = \begin{bmatrix} A^{(k)} & 0 \\ C^{(k)} & D^{(k)} \end{bmatrix} \tag{A.6}$$

where$C^{(k)} \in R^{1\times n-1}$ such that $C^{(k)} = \begin{bmatrix} 1 & 1 & \cdots & 1 \end{bmatrix}$ and $D^{(k)} = [1]$.
To find $\left[A^{(k+1)}\right]^{-1}$, let

$$\left[A^{(k+1)}\right]^{-1} = \begin{bmatrix} W & X \\ Y & Z \end{bmatrix}$$

we have,

$$\begin{bmatrix} A^{(k)} & 0 \\ C^{(k)} & D^{(k)} \end{bmatrix} \begin{bmatrix} W & X \\ Y & Z \end{bmatrix} = \begin{bmatrix} I & 0 \\ 0 & I \end{bmatrix}$$

therefore,

$$A^{(k)}W + 0 \cdot Y = I \tag{A.7}$$

$$A^{(k)}X + 0 \cdot Z = 0 \tag{A.8}$$

$$C^{(k)}W + D^{(k)}Y = 0 \tag{A.9}$$

$$C^{(k)}X + D^{(k)}Z = I \tag{A.10}$$

By solving equations A.7 to A.10, we get,

$$\left[A^{(k+1)}\right]^{-1} = \begin{bmatrix} \left[A^{(k)}\right]^{-1} & 0 \\ -\left[D^{(k)}C^{(k)}A^{(k)}\right]^{-1} & \left[D^{(k)}\right]^{-1} \end{bmatrix}$$

from equation A.5, the values $C^{(k)}$ and $D^{(k)}$we have,

$$\begin{aligned} -\left[D^{(k)}C^{(k)}A^{(k)}\right]^{-1} &= \begin{bmatrix} 0 & \cdots & 0 & -1 \end{bmatrix} \\ \left[D^{(k)}\right]^{-1} &= [1] \\ \left[A^{(k)}\right]^{-1} &= B^{(k)} \end{aligned}$$

hence,

$$\left[A^{(k+1)}\right]^{-1} = B^{(k+1)}$$

QED

Thus through mathematical induction one can understand that the initial statement from equation A.4 is valid for all positive integer values of n.

A.4 Conclusion

The final solution u is found through a series of simple mathematical operations and logical comparisons. Thus, the problem can be solved without the need for a full fledged optimization solver. Further analysis reveals that irrespective of the size of the matrix L , it can be proven that its inverse is takes the form of an explicit solution as shown in Section A.3. This proof eliminates even the need for matrix inversion operations. In summary, these modifications result in an algorithm that can solve the scheduling layer problem with significantly lesser complexity and computational effort.